REAL TIME CORROSION MONITORING OF STEEL BARS EMBEDDED IN CONCRETE USING PIEZO-ELECTRIC SENSORS

A Thesis

Submitted in partial fulfillment of the requirements for the award of the degree

of

MASTER OF TECHNOLOGY

in

CIVIL ENGINEERING

With specialization in

STRUCTURAL ENGINEERING

Under the supervision

of

Dr. Saurav

(Assistant Professor)

by

AISHWARYA THAKUR (182652)

to

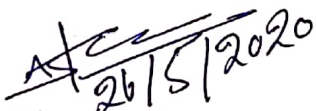

JAYPEE UNIVERSITY OF INFORMATION TECHNOLOGY

WAKNAGHAT, SOLAN – 173234

HIMACHAL PRADESH, INDIA

MAY 2020

STUDENT'S DECLARATION

I hereby declare that the work presented in the M.Tech Thesis entitled **"Real time corrosion monitoring of steel bars embedded in concrete using Piezo-electric sensors** "submitted for partial fulfillment of the requirements for the degree of Master of Technology in Civil Engineering, with specialization in Structural Engineering at **Jaypee University of Information Technology, Waknaghat,** is an authentic record of my work carried out under the supervision of **Dr. Saurav, Assistant Professor.** This work has not been submitted elsewhere for the reward of any other degree/diploma. I am fully responsible for the contents of my M.Tech Thesis.

26/5/2020

Signature

Name: Aishwarya Thakur

Roll No: 182652

Department of Civil Engineering

Jaypee University of Information Technology, Waknaghat

CERTIFICATE

This is to certify that the work which is being presented in the thesis titled "**Real time corrosion monitoring of steel bars embedded in concrete using Piezo-electric sensors**" in partial fulfillment of the requirements for the award of the degree of Master of Technology in Civil Engineering with specialization in "Structural Engineering" and submitted to the Department of Civil Engineering, **Jaypee University of Information Technology, Waknaghat** is an authentic record of work carried out by **Aishwarya Thakur(182652)** during a period from July 2019 to May 2020 under the supervision of **Dr. Saurav, Assistant Professor**, Department of Civil Engineering, Jaypee University of Information Technology, Waknaghat.

The above statement made is correct to the best of our knowledge.

Date: - …………26-5-2020…………………

HOD
CE DEPT

Signature of Supervisor   Signature of HOD

Dr. Saurav   Dr.Ashok Kumar Gupta

Assistant Professor   Signature of HOD

Department of Civil Engineering   Department of civil Engineering

JUIT, Waknaghat   JUIT,Waknaghat

ACKNOWLEDGEMENT

I take this opportunity to acknowledge all those who were a great sense of support and inspiration thought that the thesis work successful. First of all I would like to thank almighty God, my parents and many of people who have inspired and supported me, worked for me in every possible way to provide details on various related topics, and thus to make the thesis and success of the report. I thank our Head of the Department Prof. (Dr.) Ashok Kumar Gupta for his advice, encouragement and support.

I am very grateful to Dr. Saurav, Assistant Professor, for all his diligence, guidance, encouragement and support throughout the period of thesis, which enabled me to complete the thesis work on time. I would also like to thank him for the time he has spared me for his extreme busy schedule. His insight and his creative ideas are always the inspiration for me during the dissertation work.

Aishwarya Thakur
(182652)

ABSTRACT

Reinforced concrete (RC) is a very useful composite and on the list of absolute most commonly used substances in modern constructions. Reinforced concrete might also be employed in a huge selection of applications such as; construction of slab, walls, beam, column, foundation, and framework structure. Reinforcement is usually placed in areas of the concrete which are very likely to be subject to stress, as the lower portion of beams. Generally, the usage of this concrete is innovative; and, based on their support and surroundings, reinforced concrete structures can withstand decades ahead of the corrosion of steel starts. Corrosion of this reinforcement is a severe problem; it may influence the integrity and endurance of the construction. Primarily, it creates a physical barrier which prevents the steel by calling the surroundings. And another is that it gives a very alkaline environment where steel isn't vulnerable to rust. After building, concrete is subjected to a lot of surroundings throughout its service life. As soon as we focus in environment comprising chlorine, it doesn't influence concrete but corrodes steel reinforcement. For the production of steel reinforcement, then it has to be hauled through concrete. The moment the threshold for chlorine ions reaches the surface of the metal, corrosion starts. Numbers of researches are being conducted in the field of corrosion detection, as corrosion is the main reason of structural damage.

Normally, the condition of structure is tracked only through visual examination, but essential steps are taken when situation gets quite dangerous for structure. To be able to keep the corrosion levels under control, an impactful monitoring system is must and structural health monitoring (SHM) using EMI techniques is one of them. Structural Supervision (SHM) intends to create automated systems for its continuous observation, review, and detection of structural damage along with minimal labour. The very first part of setting your SHM process is to allow a degree of structure detection capability that's reliable and it has long-term equilibrium. Intelligent detection technologies, like using fiber optic sensors, piezoelectric sensors, magneto-strictive sensors and fiber-reinforced composites using self-diagnostics, have extremely crucial capacities for tracking various chemical or physical parameters connected with health insurance and, thus, a well-balanced support life of structures. Ergo, intelligent detection technologies are available and may be properly used to get health condition of construction structures. This

article critically examines the utilization of smart substances / sensors for computer construction structures. The focus is on analyzing lab and field studies of smart substances / sensors in building structures. Even though the EMI technique is a recognized technique for damage quantification and its detection.

This thesis introduces a corrosion valuation version of distinct large grades of concrete working with the impedance-based technique via the piezo-sensors. Additionally, the compression test results of three distinct grades of concrete were researched. The corrosion evaluation models are manufactured according to an accelerated corrosion analysis completed on concrete specimens. Accelerated corrosion tests have been conducted so as to acquire the information in a reasonable timeframe to get a laboratory-based study. Firstly, for compression test, total 27 cubes of three grades (i.e., M40, M50, M55) were tested. Specimens were analyzed after curing of 7 days, 14 days and 28 days for determination of compressive strength. For every grade, 3-3 cubes were divided into three batches (i.e., Batch 1, Batch 2 & Batch 3). Compression test results of each grades were equated to find out the maximum average compressive strength. The continuous load was applied at a constant rate, thus stress increases.

The research was further extended to the equivalent structural parameters for different high grades identified by the PZT sensor. Individual admittance signatures of Grades M40, M50 and M55 were recorded by using oscilloscope. Amplitude waves for each grade were recorded at 10hr, 30hr and 50hr. Further, the amplitude signatures of each grades were compared and suggested the best practically suitable grade of concrete in real scenario. The experimental results indicate the identical parameters and the developed models are successful in detecting and measuring the rebar corrosion in a sensible way. It's anticipated that this research will offer a new alternative experimental technique and a well-refined comparative result of different grades of concrete to the researchers and diagnostic engineers working within the industry of rebar corrosion.

Keywords: Oscilloscope, sensor, admittance, damage quantification.

TABLE OF CONTENTS

LIST OF ABBREVIATIONS

AE	Acoustic Emission
CA	Coarse Aggregates
CS	Compressive Strength
EMI	Electromechanical Impedance
EN	Electrochemical Noise
FA	Fine Aggregates
FBG	Fiber Bragg Grating
GPM	Galvanostatic Pulse Method
GPR	Ground Penetrating Radar
HYD	High Yield Deformed
LPR	Linear Polarization Resistance
OCP	Open Circuit Potential Monitoring
OPC	Ordinary Portland Cement
OPC	Ordinary Portland Cement
PZT	Lead Zirconate Titanate
RCC	Reinforced Concrete
RMSD	Root Square Deviation
SCC	Stress Corrosion Cracking
SG	Specific Gravity
SHM	Structural Health Monitoring
SSD	Saturated Surface Dry

LIST OF FIGURES

LIST OF TABLES

CHAPTER 1
INTRODUCTION

1.1 General

Concrete structures built around the world are dependent upon a wide scope of states of utilization and presentation to natural conditions, including corrosion, impact loads, climate conditions and pollution. These variables, alongside the implicit quality incorporated with the structure, indicate that the initial deterioration time may differ. Safety systems are intended to give a boundary among concrete and its environment, as well as the operational requirements forced on the structure. The barrier will enlarge the time until the initial deterioration. Concrete gets its strength from hydration products mostly through the C-S-H gel. The property of the concrete that made it popular is its ability to withstand compressive stresses [1].

The structure are made arrangements for long life, yet during the life of the reinforcing steel is corroded due to numerous elements that decrease stability and sometimes building can collapse. These are a few sorts of outside or mechanical variables that influence concrete failure, for example when we limit its movement, abrasion, drying and moisture, freezing and softening, overloading, structural alteration, settlement and resistance to fire. As a very important part of construction, reinforcement steel plays an important role, it prevents the bending of structure from stresses and other forces. Because concrete is resistant in compression but tension sick. Accordingly, reinforced concrete (RCC) is that concrete that can take two stresses viz pressure and ductile.

Due to the exposure of RCC structures to the distinct types of envirenment that affect the maintenance of the RCC causing damage that leads to initial losses and commercial losses [1]. One of the main deteriorations of the RCC is when the embedded steel corrodes. This reduces the axial quality and bending of the components, making them fundamentally powerless. Although corrosion of built-in steel bars cannot be seen from outside the structure and structure may seem stable, but in reality, corroded structures become vulnerable to design loads (extreme loads), for example, solid ground movement can build stress activities beyond the section boundary. Strength loss can occur in solid reinforced and steel structures. We can see in most of the time, RC structures are strong and tough, working well during their lives. However, in some cases, they don't work appropriately because of a few explanations and corrosion of the steel

rebar is one of the main reasons. As, corrosion in the steel bar is the most significant reason for disintegration of RC structures overall [2].Corrosion of metal constructions occurred extensively in numerous industries, together with oil and gas, civil infrastructure, aerospace, mechanics, mining and processing. Corrosion problems can represent a genuine danger to the security and maintenance of facilities during operation and could bring about economic loss and even loss of life in serious circumstances. As per a report by the World Corrosion Organization, the cost of corrosion is expected to be $2.5 trillion worldwide [3].

Corrosion is an electrochemical response which is originated from the iron-based metal when it comes in the exposure of environment, which is the cause of material deterioration. Due to the corrosion in steel rebars cracks are initiated in concrete. Corrosion constructed a passive film shaped in the surroundings around steel rebars because of the highly alkaline. Two conditions can break the uncomplicated condition encompassing the rebar without assaulting the solid itself, one is the chloride assault and the other is carbonation [4]. Erosion of the rebar is typically joined by the loss of the cross-sectional fragment of the rebar and the social occasion of consumption items, which understand a considerably better volume than the original steel, as such making pressure stresses, prompting breaks and solid unrests, routinely known as solid disease [5]. After some time, this issue decreases the strength of the affected structure because of the loss of bonding action among steel and solid, which eventually leads to loss of repairs. Economic losses and injure from consumption of steel bars in RC structures are supposed to be the biggest foundation problem facing industrialized nations [4]. Because of which, repair costs are a significant part of current infrastructure spending.

In modern times, Structural Health Monitoring (SHM) is well known to improve the wellbeing and dependability of facilities and in this way reduce their operating costs [6]. Quality control, support and making arrangements for the reinstatement of these facilities require non-destructive examinations and observing methods that distinguish corrosion at an beginning time. Different electrochemical and non-destructive techniques are accessible for corrosion detection and to find out the corrosion rate of the rebar. Conventional corrosion detection techniques dependent on electrochemical standards consist of potential estimations, alternating between impedance current gravimetric (mass loss), spectroscopy and direct polarization techniques.

Notwithstanding, this methodology are influenced by a number of elements. As a result, it is necessary to develop a sensation strategy to review the structure in real time (to complement routine inspections) with the goal that corrosion can be identified and treated before a major crack creates. In this research work we have utilized Ordinary Portland Cement (OPC) of Grade - 43 for the concrete mix design. On another side Geopolymer Concrete was casted and corrosion monitoring was investigated. Corrosion monitoring results of OPC Concrete was Geopolymer concrete was compared. Purpose of this comparison was to find out which type of concrete design is less prone to corrosion. And which design is more suitable for real time usage where corrosion is the main concern of that particular structure. This thesis is focused towards this objective.

1.2 What is corrosion?

Corrosion could be the attack which may damage a material of its surroundings. Corrosion can be an all process that changes to some substance in an extra form that is stable, as a sulphide, oxide, hydroxide, or even instance. It's the slow destruction of substances (typically metals) of chemical or electrochemical response by making use of their environment. The arrangement of iron oxides can be an outstanding instance of electrochemical corrosion. Corrosion can occur in substances aside from metals. For example, polymers and ceramics [8]. Corrosion affects the helpful properties of materials and structures, including fluid and gas resistance, appearance and permeability.

1.2.1 Type of corrosion

a) *Uniform Corrosion*

In this type of corrosion, a uniform and consistent decrease in thickness over the whole surface of the metal occurs. The uniform corrosion rate can be effectively controlled by measuring mass loss or the amount of hydrogen discharged [9].

b) *Localized Corrosion*

Localized corrosion is located expressly organized in an area with a metal surface. Localized corrosion is an accelerated attack of a passive metal in corrosive surroundings. General types of

localized corrosion include intergranular pitting corrosion of an alloy with a susceptible grain limit region and analytical localized corrosion showing. Localized corrosion happens when working with other damaging processes for example stress fatigue, corrosion and different types of chemical assault
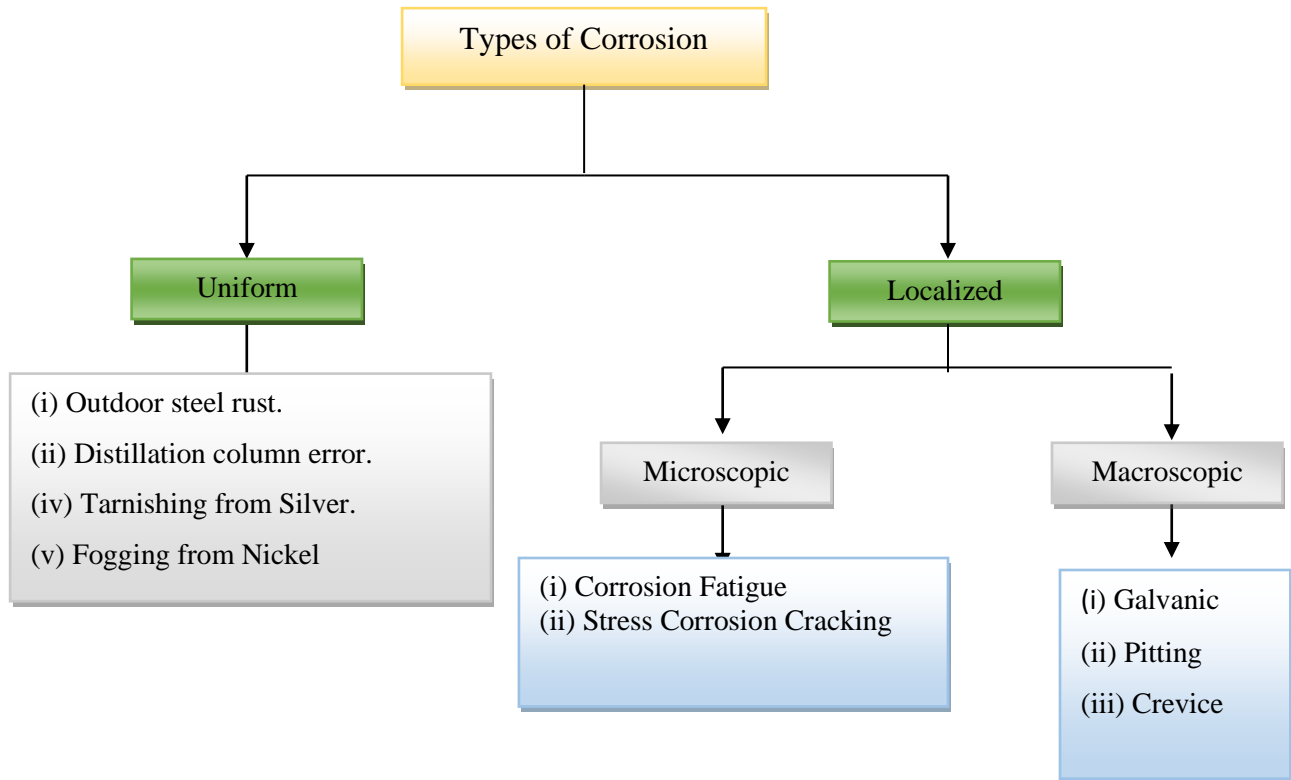
Figure 1.1: Type of uniform and localized corrosion

Type of Localized Corrosion:

 i. Galvanic Corrosion:

Galvanic corrosion is additionally called bimetallic corrosion. When two unconnected metals have physical or electrical contact with one another and are submerged in a typical electrolyte then galvanic corrosion happens. In a galvanic pair, the most dynamic metal (anode) corrodes at an accelerated rate and the noblest metal (the cathode) corrodes at a moderate pace. Galvanic corrosion influenced by metal types, relative size of anodes, and working conditions (temperature, humidity, saltiness, etc.) influence [10, 8]. The surface proportion of anode to clearly influences the corrosion rates of the material.

ii. Pitting Corrosion:

Pitting corrosion is a localized assault wherein corrosion dissolved the metal, forming gaps or pits. This kind of corrosion is risky because it is complicated to identify due to corrosion items that can cover wells, which are not easy to plan against well development, just as predict when this form of corrosion can happen [10]. Pitting corrosion is regularly detected in passive metals and alloys such as aluminum composites and stainless-steel alloys when the ultra-slim oxide film (passive film) is mechanically or chemically damaged and isn't quickly passive again. The subsequent wells can turn out to be wide and shallow or shallow and deep that can rapidly penetrate the thickness of a metal wall [11].

iii. Corrosion Fatigue:

Pitting was seen as related with constituent particles in the gap and pit development frequently included blend of individual molecule nucleated pits. Fatigue splits are regularly nuclearized by a couple of the greatest wells, and the size of the pit where the fatigue break assembles is a segment of the stress level and load frequency. When there is a joint movement and cyclic load, there is occurrence of degradation in material. Excellent structure materials around has a significant role in the weakening of material, for instance, aluminum alloy, steel and titanium alloys. It depends upon the relations between the load, environmental and metallurgical elements.

iv. Crevice Corrosion:

Crack corrosion refers to the attack on the metal surface or directly adjacent to the gap that connects two retaining surfaces. The void or slit can form between two metals or a metal and non-metallic materials. Out of the hole or without the gap, the two metals are corrosion resistant. Damage caused by break corrosion is normally constrained to a metal in the area on or close to intersection surfaces [9].

v. Stress Cracking

Growth of crack in a corrosive environment is termed as Stress Corrosion Cracking (SCC). It causes an amazing unpredicted disappointment of generally ductile metal alloys under tension, particularly at high temperatures. SCC is very chemically specific as some alloys are probable to change from SCC when introduced to a minute number of chemical environments. The chemical surroundings that SCC causes for a specific alloy is frequently one that is just slightly corrosive to the metal. Hence, metal parts with genuine SCC can show up bright and shining while at the same time being charged with microscopic slits. This is an important factor for SCC to get unnoticed before collapse. SCC is progressing quickly and is more typical in alloys than in pure metals. The definite surroundings are essential, and extremely low absorptions of some highly active chemicals are said to make disastrous cracks, which frequently lead to devastating and unanticipated disappointments [13].

Uniform

Galvanic

Pitting

Fatigue

Stress- cracking

Crevic
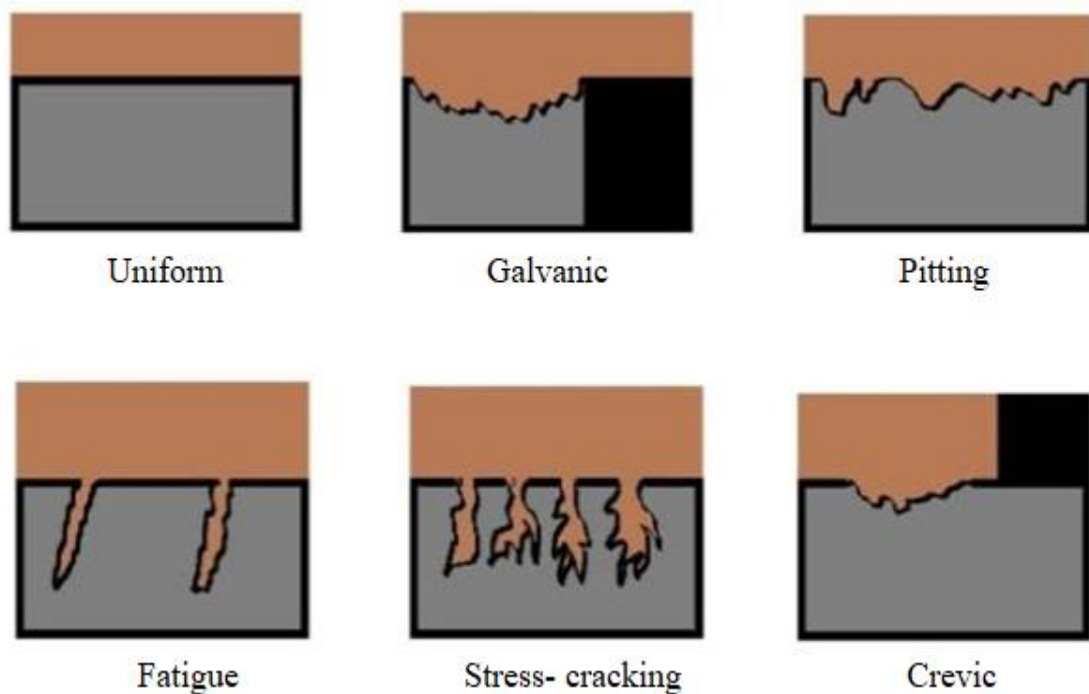
Figure 1.2: Different types of corrosion [10]

6

1.3 Mechanisms of corrosion steel

Corrosion of steel in any surroundings is a process that incorporates the dynamic evacuation of iron atoms (Fe) from corroded steel. The iron is cleared by an electrochemical response and dissolved in the close by water solution, showing up as ferrous ions (Fe^{2+}). In embedded concrete steel, dissolution happens in the pores of the concrete when restricted volume of water solution present in the surrounding the steel. Due to the dissolution steel loses its mass, for instance, its transverse region decreases. If steel is part of reinforced concrete structures under load, the tension of the cross segment that is maintained will increase fundamentally. In extraordinary cases, for example, the increase can pose a security risk or even cause an error. This is one of the undeniable dangers related with steel corrosion in concrete.

Dissolved iron ions in concrete pore water arrangements ordinarily react with hydroxide ions (OH^-) and dissolved oxygen molecules (O_2) to show one of a few assortments of rust, which is a solid element for corrosion response. Oxide is normally stored in space tied to concrete around steel. Its development within this confined space has made expansive tensions that can break the concrete roof. This in turn can cause the dynamic decomposition of concrete, especially when freezing and thawing or other environmental impacts prevail.

1.3.1 Corrosion reaction (Anodic and Cathodic reactions)

Corrosion within steel inserted into concrete is termed as electrochemical method. The surface of corrosive steel acts as a mixed electrode which is a compound of electrically related anodes and cathodes through the steel body, where anodic and paired cathodes are formed. Concrete pore water acts as a liquid medium, in other words, a complicated electrolyte. Along these lines, a corrosion product is formed as shown in the Figure 1.3.

Response values are often referred to as half-cell responses which were taken from anodes and cathodes. The "anodic reaction" is that the oxidation process, which causes the disintegration or reduction of metal; whereas the "cathodic reaction" is the procedure of decrease that result in the decrease in the hydroxyl ions of the dissolved oxygen arrangement [14]. For embedded concrete steel, coming up are potential anodic reactions that rely on the pH of this interstitial electrolyte, the nearness of the beveled anions along with the attendance of sufficient electrochemical potential on the surface of the steel.

7

$$3Fe + 4H_2O = Fe_3O_4 + 8H^+ + 8e^- \tag{1.1}$$

$$2Fe + 3H_2O = Fe_2O_3 + 6H^+ + 6e^- \tag{1.2}$$

$$Fe + 2H_2O = HFeO_2^- + 3H^+ + 2e^- \tag{1.3}$$

$$Fe = Fe^{2+} + 2e^- \tag{1.4}$$
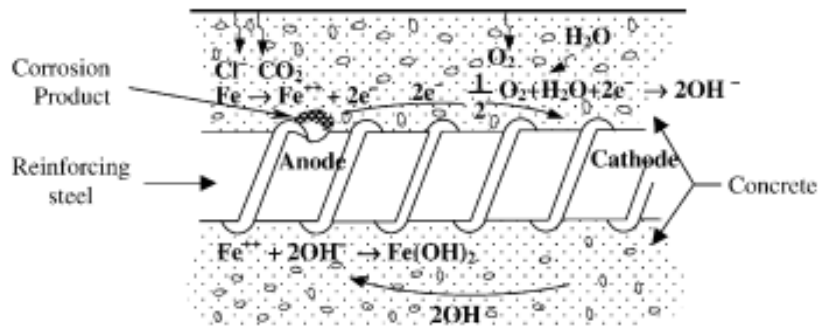
Figure 1.3: Schematic figure of corrosion in reinforcement steel [14]

Possible cathode responses rely upon the accessibility of O_2 and pH in the region of the steel surface. The most possible responses are:

$$2H_2O + O_2 + 4e^- = 4\ OH^- \tag{1.5}$$

Or

$$2H^+ + 2e^- = H_2 \tag{1.6}$$

1.4 Causes of corrosion

1.4.1 Carbonation of concrete

The carbonation rate is basically physically restricted by the carbon dioxide diffusion process and chemically by the concrete calcium hydroxide stock. Carbon dioxide spreads from the environment into the capillary pores of concrete and is joined with carbonic acid, which at that point responds with alkaline hydroxide, sodium, potassium and calcium, forming carbonates

[15]. Since the concentration of calcium hydroxide in ordinary concrete is normally higher than the concentration of other hydration items, the CO_2 response with $Ca(OH)_2$ predominates and the carbonation process can be described essentially by the accompanying compound response:

$$CO_2 + Ca(OH)_2 \xrightarrow{H_2o} CaCO_3 + H_2O \tag{1.7}$$
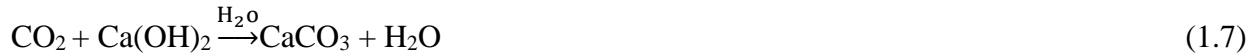
The distance from concrete is the depth of carbonation where alkalinity of cement decreases. A carbonation front happens exclusively as per the laws of dissemination. The depth of carbonation depends upon the product of coefficient and square root of time.

$$x = K\sqrt{t} \tag{1.8}$$

wherever,

X= Depth of carbonation,

t = Time

K is coefficient of diffusion.

Here K depends on the temperature, nature of the concrete. Depth of carbonation relies on the quality of concrete. The depth of carbonation can dictated by different procedures. Since carbonate diminishes pH. Through pH markers we can utilize the concrete assurance, for instance, the phenolphthalein on a newly cut or lately broke concrete surface to assess the depth of carbonation. Right when phenolphthalein is applied, non-carbonate portions are red or purple, while carbonated areas are colorless. At a pH of 9.8 or higher, the maximum color change to deep purple red happens. Pink colour shading appears below 9.8 and colorless at pH of 8.

1.4.2   Chloride induced corrosion in concrete

Among the most common reasons due to which corrosion occurs in concrete structure is the bonding of chloride particles. They induce the localized break of this inert film that creates mostly around the steel due to the alky nature of the concrete pore arrangement [16]. The most critical corrosive agents, for example, chlorides, can go inside the concrete from many resources. From contaminated mixing elements a strong chloride ion can instigate (provide concrete as a groundwater newspaper/seawater from the contaminated combination of aggregates or because of splashes of sea salt/lead wetting or deicing salt) from the brand-new state or by the nearby surroundings from the hardened state. Alkalinity of the pore arrangement decreases when

chlorides diffused in concrete (in the first pH.13 to over 7) after corrosion [14, 17]. In earlier times it's been believed the outset of corrosion occurs when the concentration of chloride at rebar level arrives at an essential level, which can be also frequently known as the threshold level.

1.5 Structural health monitoring

The facilities are usual or special; these are valuable parts and are simply connected with living and non-living creatures. Now and again a minor deformity inside the structure could influence the whole body and lead to fall down of the structure that could make a huge loss of property and humans as well. Along these lines, expanded responsiveness of this monitoring technique and also provides a solution for the affected structures due to ageing. People the day preceding just utilized a visual inspection to sense defects, but extraordinary and worse damage to infrastructure prompts to the development of new technologies for the acknowledgment of new methods of structural health monitoring as damage detection tools. Various sorts of sensors are associated with the computer system along with special hardware and software that gives the mark and helps to underline the hazard zone. To recognize and calculate the corrosion rate of rebars in RC structures, a number of electrochemical, destructive and non-destructive methods are accessible, in brief described beneath [18].

1.5.1 Methods of SHM

a) *Destructive method:*

In destructive tests (or in destructive physical investigations, DPA) are performed for sample failure so as to understand the presentation of a sample or the performance of the material under various loads. In this technique, the sample is broken to decide physical and mechanical properties, (for example, strength and ductility). The types of destructive tests are fractures and mechanical tests, fatigue tests, hydrogen tests and residual stress estimation.

b) *Non-destructive method:*

Non-destructive testing methods are frequently applied in industries where part failure would cause significant risks or economic losses, such as transportation, pressure vessels, construction

structures, pipes, and lifting equipment. In this method we find out the characteristics of the material to sense the defect without destroying the material.

Table 1.1: Non-Destructive methods

No	NDT Methods	Principles	Merits	Demerits	Corrosion Evaluation	Specific Tools
1	**Electrochemical method [19]**					
	Resistivity method	RC resistance, which current can simply switch connecting areas of anode and concrete cathode.	A straightforward, quick, compact and economical method, which can be utilized for routine inspection.	Reinforcement in the test zone can give a way of "short circuit" and cause a wrong estimation decrease.	Resistivity (Ω cm).	Current and potential electrode, volt units or resistance and insulation cable (working electrode).
	Open circuit potential (OCP) monitoring	The open circuit voltage (OCV) refers to the entire electrochemical cell and the capacity of the open circuit to an electrode. This measure is intended to record the progress of the potential of the rest, e.g. when no current flow flows through the cell and a potential is applied to the electrode against a reference electrode or a potential contrast is applied to the cell.	The results are not also equivalent contours, but a unique value that gives a sign of the state of the steel.	It requires long time and must be closed for a number of hours throughout the inspection**.**	Potential level (mV or V).	Potential electrode, Voltmeter, and interfacing cable (working electrode).
	Polarization resistance [20]	The estimation of the linear polarization resistance of steel in concrete is regularly used to assess the kinetics of steel dissolution inside a proven corrosion area.	Short time for estimation and applies little disturbances that don't interfere with existing electrochemical procedures.	It requires some investment to get a total reaction because of electrical limit through the steel and concrete border. The voltage fault introduced by the IR drop of	Corrosion current (I_{corr}) (A/cm^2). .	Reference electrode, counter electrode, voltmeter, ammeter and connecting cable (working electrode). (Deby, F. (2018))

				the concrete along with the work (steel bars) and the suggestion electrode.		
	Galvanostatic pulse method (GPM)	GPM corrosion evaluation depends on the existing measurement wanted to change the potential dissimilarity between the reinforcement and a standard reference electrode [21]. The current is a result of electrons from the anodic and cathode sides in concrete.	Simple to learn, requiring a medium-low level of experience for equipment configuration and information collection.	Unstable estimations when resistance to concrete cover is high.	Potential resistance (Rct) (kΩ·cm^2)	Reference electrode, counter-electrode, security ring and associating cable (working electrode).
	Electrochemical noise (EN)	Electrochemical noise (ECN) is the non-exclusive term for fluctuations in current and potential. In connection with corrosion, it is the result of the adjustment of the current pulses generated by the unexpected breakage of the film, the crack propagation, discrete events with the dissolution of metals and hydrogen exhaust gases with the arrangement and detachment of gas bubbles.	Simple to utilize, no system interference and estimated signs can be analyzed utilizing numerical examination.	Complicated kinds of noise (for example physical origin) because of steel reinforcement corrosion make numerical investigation unproductive.	Noise resistance (Rn) (kΩ·cm2).	Electrodes (reference, counter and work), voltmeter, ammeter, amplifier and data capture card.
3	**Optical sensing method**					
	Fiber Bragg grating (FBG)	The change in the FBG wavelength measures the increased in fiber stresses with an increased in the cross section of the steel reinforcement of corroded RC structure.	Displays a liner response when measuring voltage, pressure and temperature.	It's expensive to build and maintain.	Bragg wavelength (λB).	Fiber optic sensor, Bragg meter and computer.
4	**Infrared thermography method [22]**					

	Infrared thermography (IRT)	IR radiation produced by a concrete material is changed over into an electrical signal and handled to make surface temperature maps.	Easy explanation of results and without radiation, quick setup, portable and helpful method.	There is no quantitative information on corrosion damage (e.g. size or depth).	Radiation power (E)	Multi spectrum camera.
5	**Elastic wave method [23]**					
	Ultrasonic pulse velocity (UPV)	When the pulse is induced into the concrete by a transducer, it is subjected to multiple reflections at the limits of the different material stages inside the concrete.	Concrete testing equipment utilizing ultrasonic pulses gives faster and progressively exact results.	A high level of ability and operator integrity is required. Subsequently the requirement for trained and certified NDT personnel.	Pulse velocity (V).	Transducers (transmitter and receiver), amplifier, and oscillator.
	Acoustic emission (AE) [24]	Acoustic emission can be characterized as a transient elastic wave created by the rapid release of energy inside a material.	It can recognize harm to defects that are hard to access with conventional non-destructive testing methods.	It might be more slower than other non-destructive testing methods.	AE parameter.	Transducer, preamplifier, filter, amplifier, and storage equipment.

1.6. EMI technique using Lead Zirconate Titanate (PZT) patches

1.6.1 Working Principle

From this impedance technique, a piezo-patch has been attached into the top layer of the structure to be tracked with non-metallic epoxy glue and excited through a capability to induce resistance Meter (LCR). Within this setup, the PZT patch basically acts like a lean plate exposed to axial vibrations along with getting together with all the host structures, as shown in Figure 1.4 (a & b) and those interactions have been represented in the sort of electrical entrance contains conductance along with suseptance. Let's assume that the 1 D interaction (host structure like PZT patch host structure might be modeled as a (as a result of host structure) attached with a lean pub

(patch), Figure 1.4(a). The piezo-patch expands and contracts towards '1' in which an E3 alternate electrical field (that can be spatially uniform, such as $\partial E3 / / \partial x = \partial E3 / / \partial y = 0$), uses from side '3'. The patch includes 'l' in half a width 'w' and depth 'h'. Effects can be mathematically expressed as

$$D_3 = \overline{\varepsilon_{33}^T} E_3 + d_{31} T_1 \tag{1.9}$$

$$S_1 = \frac{T_1}{\overline{Y^E}} + D_{31} E_3 \tag{1.10}$$

Here axis '3' factors alongside the thickness of the patch as shown in Figure 1.2 (a).

Here,

S_1 represents the strain along axis '1',

D_3 represents electrical displacement on piezo-patch surface,

d_{31} represents the coefficient of electrical deformation

T_1 represents the axial stress on the patch

$\overline{\varepsilon\varepsilon_{33}^T} = \varepsilon\varepsilon^T{}_{33} (1 - \delta j)$ is electrical permittivity

η mechanical loss factor and

δ indicating the dielectric loss factors of the patch separately.

$\overline{Y^E} = Y^E (1 + \eta j)$ is the Young's modulus of elasticity.

(a)   (b)
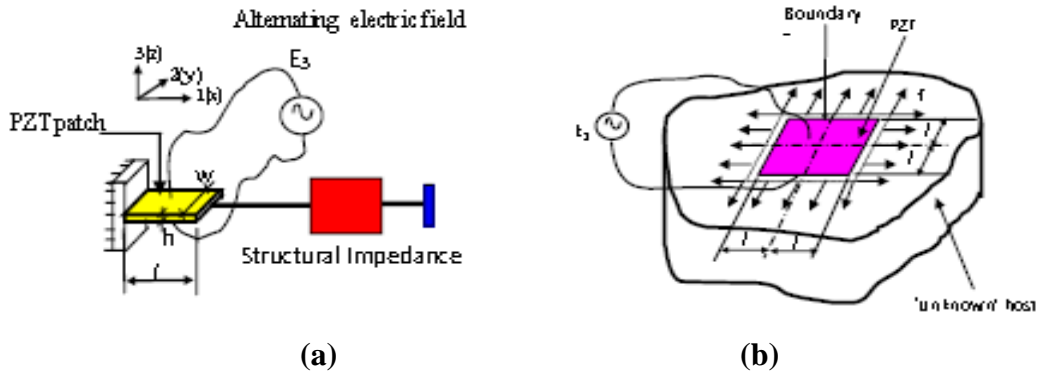
Figure 1.4: Interaction of PZT Patch (a) Structure of PZT modelling (1D) (b) Host structure bonded with PZT patch (2D) [66]

Therefore, it can be assumed that the structure has a uniform dynamic rigidity for attached part. So this is expected that there is equal mechanical impedance at the last two points. In these conditions, the PZT patch takes zero midpoint (x=0), regardless of the position of the patch in the host structure. Based on these predictions, the vibrations of the 1D patch can be characterized by the given derivative based on the dynamic balance of the PZT patch [66].

$$\overline{Y^E} \frac{\partial^2 u}{\partial x^2} = \rho \frac{\partial^2 u}{\delta x t^2} \tag{1.11}$$

Here 'u' represents displacement at anywhere in the patch in the '1' direction. The solutions adjust the differential equation with the technique of separating variables and limits conditions compatible with previous conventions.

$$u = A\sin(kx)e^{jwt} \tag{1.12}$$

Here,

k is the wave number,

ω is angular frequency,

ρ is the density.

$$k = \omega \sqrt{\frac{p}{Y^E}} \tag{1.13}$$

Getting the most of this PZT connection (Eq. 1.13), also incorporating through the full outermost layer of the PZT patch (0 + l), we could get an expression to its Electro Mechanical admittance (the reverse of electro mechanical impedance) as

$$\overline{Y} = \omega j \frac{wl}{h} \left[\overline{\varepsilon_{33}^r} + \left(\frac{Z_a}{Z + Z_a} \right) d_{31}^2 \overline{Y^E} \frac{\tan kl}{kl} - d_{31}^2 \overline{Y^E} \right] \tag{1.14}$$

Where, Z_a is the short-circuited mechanical impedance of the PZT patch, given by

$$Z_a = \frac{kwh\overline{Y^E}}{(j\omega)\tan(kl)} \tag{1.15}$$

Z_a is described as the pressure for producing unit velocity from the PZT patch in short-circuited conditions (i.e., dismissing the PZT influence) and dismissing the host structure. It must be said that no assumptions have been made in regard to the frequency range of operating from the aforementioned equation. For your instance of $\omega \ll \omega_{res}$, when $\frac{\tan kl}{kl} \rightarrow 1$, the Eq. 1.14 reduces to

$$\overline{Y} = \omega j \frac{wl}{h} \left[\overline{\varepsilon_{33}^T} - \left(\frac{Z}{Z+Z_a} \right) d_{31}^2 \overline{Y^E} \right] \qquad (1.16)$$

Eq. (1.14) or Eq. (1.16) pairs the mechanical impedance of this mechanical system using an electromechanical admittance of this PZT structure system. The very first term of these specimens is that the skill of PZT, and also the rest conditions suggest mechanical interaction between the structure and the actuator.

The genuine one the connection between the patch and the structure isn't limited at the endpoints yet extended along the finite number of PZT patches as shown in Figure 1.4(b). Thus ensuring the transmission of pressure between the patches and the PZT structure happens along the whole limitation of this patch.

$$\overline{Y} = \frac{\overline{I}}{\overline{V}} = G + Bj = 4\omega j \frac{l^2}{h} \left[\overline{\varepsilon_{33}^T} - \frac{2d_{31}^2 \overline{Y^E}}{(1-\vartheta)} + \frac{2d_{31}^2 \overline{Y^E}}{(1-\vartheta)} + \left(\frac{Z_{a,eff}}{Z_{s,eff}+Z_{a,eff}} \right) \left(\frac{\tan kl}{kl} \right) \right] \qquad (1.17)$$

Where $Z_{a,eff}$, is the powerful mechanical failure of this structure, ϑ the Poisson's ratio. Damage to the structure (for example, corrosion, which leads to a change in the mass and rigidity of the structure) can lead to a change in the structural elements, and then to a change in the total resistance of the structure ($Z_{s,eff}$), which then changes the record ($\overline{Y}$) in the previous equation, functioning and a sign of the design's operability.

1.7 Accelerated corrosion testing

Ordinarily concrete provides great corrosion resistance due to its significant characteristic, particularly the elevated alkalinity of the artificial solution, which includes chiefly of sodium hydroxide and potassium combined with a pH ranging from 12.6 to 13.8. This passive film can develop to a thickness of 10-3 to 10-1 μm and contains sexy iron oxides. The notion of the existence of the passive coating is based on indirect signals of anodic polarization measurement. There is still much to understand concerning this passive film, such as the provisions of its own production in addition to its chemical and mineralogical composition. It is very likely this passive film includes several stages. The concrete cover also provides excellent physical protection to the steel chloride ions and also avoids carbonation. Thus, the steel demands a

lengthy period to depassivate and allow the corrosion process to get started. This makes it quite difficult to replicate research and understand corrosion happenings in labs. [25].

1.7.1 Artificial Climate Technique

Inside this corrosion technique, the method is accelerated by high temperatures, higher humidity and repeated wetting and drying cycles. Artificial surroundings or environment techniques, where samples are kept in a controlled environment, are frequently utilized to accelerate the startup period. Artificial weather requirements supplied by Dimitri [26] that temperature is 40 degrees Celsius (104 degrees Celsius), (RH) Relative Humidity, 80 percent and sodium water (5% NaCl solution) spray (1 hour) and infrared light (7 hours) for drying and wet cycle. The most frequently used methods are:

(i) With 50% CO_2 and 65% Relative Humidity - Carbonation chamber,

(ii) Samples contaminated by 3-5% NaCl solution (permanent absorption).

The process of corrosion and its characteristics of the steel bar in artificial environments are much like corrosion in the natural environment. The air-conditioned surroundings as an accelerated way of lab testing are much more representative of this galvanostatic process.

1.7.2 Impressed current technique/ Galvanostatic method

Impressed current technique is used to accelerate the corrosion in reinforcing steel. The current procedure, likewise called a galvanostatic technique; steel embedded in the concrete with constant current supply is to make significant corrosion in a quick time span. After this process Faraday's law, is used to calculate induced corrosion with the assistance of a gravimetric test performed on the extracted bars after undergoing accelerated corrosion

1.7.3 Static atmosphere testing

Static environment tests are just one where a test room is used to make and maintain one surrounding during testing. The most frequently used corrosion test of its type is salt mist test (ASTM B 117). The pieces are subjected to constant surroundings of 35 or even 100% relative humidity, using a sodium chloride solution of 5 percent (by weight) atomized to get a predetermined moment. The pH of this collection alternative should be 6.5 to 7.2. The length of

the test maybe 48-2,000 hours based on the substance being tested. Despite the recent failures, the salt spray testing stays a workable quality control review tool for use after a baseline was established.

CHAPTER 02
LITERATURE REVIEW

2.1 General

In this chapter addresses with the evaluation of the literature with regards to the effects of corrosion. The corrosion has been triggered by the existing procedure and the belongings were also investigated. Literature on corrosion quantification techniques was also discussed. This chapter discusses how the studies conducted by investigators to review methodologies utilized in knowledge of results and evaluations setup. This chapter covers these results and guidelines for upcoming examination.

2.3 Literature survey

G. Park et al [28] studied the fundamentals of structural health monitoring dependent on impedance. The PZT quick model and host structure were scientifically analyzed utilizing the wave state to explain how the electrical obstacle vary in the linked PZT is related to the frequency reaction of the method at high frequencies. At the time of distribution, there was no link among the change in the electrical barrier inside the PZT and an adjustment of the mechanical properties of the system. Spectral technology was used to build up an open beam examination representation consisting of ten spectral components. The damage was caused by increasing the number of waves associated with the change in stiffness and module of the young structure. A damage locator vector indicates the damage level of each part and accurately detects the damaged segment.

The test was supplemented by the combination of several patches with a free beam, & impedance tests were performed at 70-90 kHz. Screws have been supplementary to the construction to vary the mass properties and stiff systems. This check utilized the actual part of the impedance signal was used for examination since it is delicate to the difference in nonexistent parts or else magnitudes that are capacitive and less delicate to changes. As a result, accelerometers were associated with beam reaction functions and the frequency was evaluated the longitudinal way.

The outcomes show a decent match among expository and exploratory models, which indicates the usefulness of impedance.-dependent structural observing.

D.M. Peairs et al. [29] have accumulated a minimum of effort, a miniaturized estimating instrument, to build the availability and portability of the obstruction strategy. In the past, actualizing the impedance strategy required expensive, huge and exorbitant obstacle analyzers such as HP4194A. The financially technology has replaced the obstacle analyzer with an FFT analyzer and a continuous measurement track. Since profitable equipment and programming currently enable FFT on a solitary chip, the entire arrangement can be deployed on one PC (compute) chip. The price-effective impedance strategy is adapted in an impedance analyzer & tested on pipes & complex structures to demonstrate the precision of the ease technique in genuine structures. Although this cost-effective alternative has not been tested for corrosion damage, it is a necessity for future standalone SHM devices, depending on the obstacle.

M.F. Montemor et al [30] explain that the main causes of corrosion of steel are the occurrence of chloride particles. They cause a localized break of the passive film, which was originally formed on the steel due to the alky nature of the arrangement of the concrete pores. Dangerous chloride particles can begin with the utilization of impure mixed components or the nearby atmosphere. As a first approach to the system study, the possible mapping method for detecting corrosive reinforcement was suggested. The method has proved to be appropriate to on-the-spot checking; however, the outcome must be carefully deciphered, particularly under the limited O_2 supply. Some Direct current had the option to compute the protection from polarization. The exactness of the method has been greatly improved by the utilization of estimating instruments that work according to the principle of protective ring technology. The development of portable and simple to-utilize observation systems makes the process suitable for a rapid corrosion rate on site. The transitional techniques used in the field of time have proved to be efficient meant for on-the-spot checking. These procedures are quick and non-damaging and give information on steel conditions just as data on concrete opposition. The nearness of procedures other than forms that are restricted by activation can reason deviations from the normal exponential actions, & in this way it is hard to guess system parameters, which can lead to an underestimation of the corrosion rate.

F. Hey et al [31] studied some specialized issues regarding the execution of electromagnetic impedance (EMI) technique established Structural health monitoring and suggested latest sensors examination calculations using the sensor multiplexing method to decrease the era demanded in examining lead zirconate titanate (PZT) fixes one by one. Any alteration in the bulk, stiffness, or damping of the structure (because of damage) would lead to a shift in the admittance touch of the lead zirconate titanate (PZT) fix. The admittance touch of the PZT fix is readily gotten using any industrial impedance analyzer.PZT patches have rapid responses and have the capacity to behave as collocated sensor and actuator, thus cutting down the amount of apparatus along with the affiliated wiring. Mostly, the problems addressed were the various signature processing tools out there for calculating of damage localization, usage of a parallel investigation technique, security of sensors, and observation of concrete curing. During application of concurrent investigation, the investigation time could be significantly diminished. The damage localization algorithms performed quite satisfactorily concerning optimizing the time necessary for damage localization and also the truth of the found damage.

J. Yang et al [32] studied nearby corrosion of the steel bar in the aquatic surroundings, and an investigation dependent on the electro-mechanical impedance is conducted. The corrosion form of the steel structure is separated into unvarying corrosion and nearby corrosion. Lately, the PZT as an intelligent substance has been generally utilized for structural health monitoring (SHM). For damage to local corrosion in the appearance, a research was designed to observe nearby corrosion of the steel bar dependent on the EMI technique. The oceanic condition was recreated and local corrosion state of the steel beam was designed first. The PZT surface transducer was then utilized in the structure for long-standing observing. The corrosion advancement procedure and the difference of intake has been the subject of examination. The result shows that the electromechanical impedance technique is accessible to monitor local bar corrosion via examining the input signal modification law and the resonance frequency deviation percentage list with steel bar corrosion.

H. A. Dehwah et al [33] has investigated that reinforcement steel corrosion is a major sustainability problem worldwide. The long periods associated with the replication of rebar corrosion within the research centers have led to the improvement of several accelerated testing

21

methods. The research presented in this article was based on the study of the current imaging technique, which is regularly used to induce corrosion reinforcing. When a pressure current is utilized to generate corrosion, the quantity of mass loss is connected to power consumption as soon as passivity is impaired, and can be modeled with the Faraday Act, Equation (1)

$$\text{Mass loss} = \frac{Mit}{zF} \tag{1}$$

Where,

M = molecular weight (55.847 g/mol) for iron,

i= current (A),

t = time (s),

z = no. of e$^-$ transferred, and

F = Faraday's constant (96487 Coulombs/mole).

The relevance of the chloride-induced corrosion modelling technique was calculated via studying the electrochemical character of the test technique. Corrosion of the reinforcement was activated by the use of a set anodic current of 100 A/cm^2 to the prism. The electrochemical potential of the steel was monitored with a saturated calomel reference object on the surface of the concrete. Because of the effects of the voltage apply to the potential erosion was constantly checked with the new AE (Acoustic Emission) technology. At the end of the study, the prisms were outwardly inspected for surface cracks and a visible assessment of the eroded surface was carried out. The gravitational mass trade was noted after the protection was expelled from the prism and wiped. The RC (Reinforced concrete) was launched with planned characteristics of 20MPa, 35MPa and 50 MPa. Every mixtures contained uncrushed waterway rock with a most extreme all out size of 10 mm and had a free water content of 180 kg/m^3. AE technology was valuable and dependable in identifying the occurrence of corrosion. This vision was carried by a decent expectation of mass loss via the Faraday's Act, considering the inactive period demonstrated by the estimation of the AE.

W. Li et al. [34] investigated a proposed new corrosion monitoring method based on lead-zirconate-titanate (PZT) based smart corrosion coupon (SCC) utilizing electromechanical impedance (EMI). The main thinking of the corrosion monitoring method was that the loss of

thickness caused by SCC corrosion will lead to fluctuations in EMI signatures. The SCC was a corrosion coupon with a PZT patch. Five SCC models were manufactured in the research facility, which is marked by SCC1 to SSC5, as appeared in Figure 2.1. The PZT patch had a diameter of 8 mm & a thickness of 0.45 mm. The EMI signatures of the SCC were rehabilitated and examined with various corrosion. The results showed that the tips of the lead signatures changed to the left and the peak frequencies decreased linearly as the amount of corrosion increased. For more information about the electromechanical SCC system, an analysis of the finished elements was also carried out to investigate the reaction and modal attributes of EMI. The test results were clearly in line with the test results. In addition, he worked to ensure that the combined bending modes are very sensitive to the loss of thickness caused by corrosion. The proposed intelligent corrosion coupon is cost-effective, can quantitatively determine the amount of corrosion and has promising application potential.
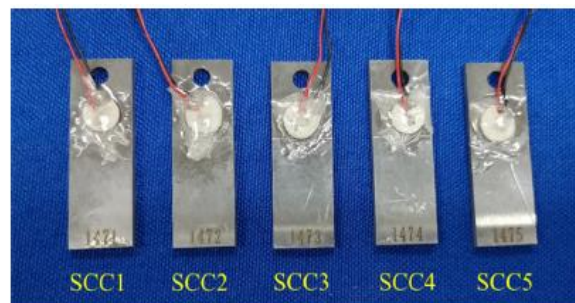
Figure 2.1: Photos of the fabricated SCC (Source: W. Li et al [34])

D. Ai et al. [35] investigated an innovative electromechanical deficiency technique (EMI) with the united mechanical impediments (UMI) of a lead-zirconium titanium sensor (PZT) and proposed a host structure for monitoring a corrosion-damaged steel beam at dissimilar times. Two PZT surface-bonded sensors were connected to the steel bar and were utilized to screen the advancement of erosion harm by identifying changes in electromechanical admittance. Admission electromechanical was estimated for the period of the 1st, 22nd, 45th & 117th days, which were utilized to check the united mechanical impediments. While calculating the frequency compensation of the resonance peaks of the united mechanical impediments curve, the deterioration of the harm can be subjectively corrected. Average root square deviation values (RMSDs) obtained from the actual division of the united mechanical impediments can be utilized

to quantitatively find out the harm degradation. For the proposed mark of the UMI, the direct relationships between frequency change and erosion time and root square deviation at the hour of corrosion were independently summed up. Comparative investigations on electromechanical approval and united mechanical impediments have shown that a united mechanical impediment is supplementary sensitive to the detection of structural damage caused by corrosion by steel. The results also confirmed that adjustments to the MI (Mechanical Impedance) of lead zirconate titanate sensors caused by structural damage to electromechanical impedance (EMI) technology must not be ignored. In summary, united mechanical impediments has proven to be a fundamentally viable EMI method for checking the structural health of steel.

B.S. Jang and B. H. Oh [36] investigate the impacts of uneven corrosion on the breaking behavior in the concrete roof. Erosion of the steel beam in the concrete can cause development weight and this expansion pressure can exert loads cracking around the reinforcement rod. The reason for this examination was to investigate the impacts of uneven corrosion on the splitting conduct of the solid roof. The split weight diminishes to about 60%, contingent on the type of uneven corrosion distribution. The inspection also showed that the pressure to crack the concrete roof by the extent of the corrosion increased with an increase in the coverage deepness and approximately linearly relative to the dia. between the ceilings (c/d). The crack pressure of the concrete layer decreased slightly with increasing diameter of the rod. Be that as it may, the impact of the bar diameter on the crack pressure because of the corrosion of the steel turns out to be quite small. The results of this investigation were compared with the crack pressure test information of the concrete cover. It is definite that the outcome of the studied study matches the test data well overall.

A. A. Almusallam [37] conducted a study to assess the effects of corrosion of reinforcing steel bars on their mechanical properties. The steel rods corroded into reinforced concrete samples with a diameter of 6 and 12 mm in dia. were removed and tested in stress. The result showed that the corrosion reinforcing stage did not affect the stress resistance of the steel rods determined on the actual surface of the cross-section. In any event, the stress resistance when using the nominal diameter was not exactly the ASTM requirement of 615 of 600 MPa when the corrosion rate was

11 and 24% respectively for steel bars 6mm and 12 mm (diameter). In addition, the reinforcement of steel rods with a corrosion of more than 12% indicates a brittle defect.

T.A. El Maaddawy and K.A. Soudki [38] studied quickened corrosion through the impressed current method that is extensively utilized in concrete toughness tests. In this research, the impact of differing the level of impressed current density range 100 & 500mA/cm2 on the real degree of erosion of the steel R/F (Reinforcement) bar and the behavior of concrete deformation because of extensive corrosion items was tentatively studied. Twelve RC prisms 150×250×300 were utilized. The prisms were R/F by two number ten rebar. Corrosion was prompted by methods of impressed current utilizing electric power supplies. The details of the test sample are appeared in Figure 2.2.
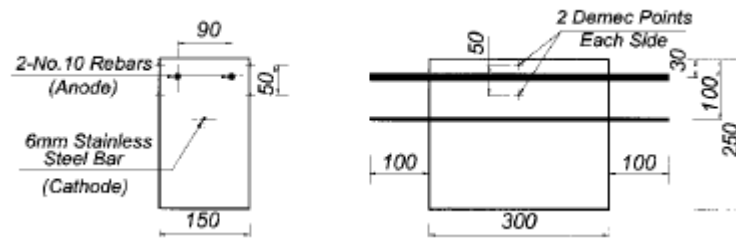
Figure 2.2: Information of test specimen (every dimension is in mm) (Source: T.A. El Maaddawy and K.A. Soudki [38])

To de-space the steel R/F, 5 percent NaCl was added via concrete weight to the cement mixture. The response to deformation because of the development of corrosion items was estimated on each side of the prisms. Toward the finish of the erosion stage, every rebar have been expelled, cleaned by ASTM G1-90 and heavy to accomplish the real level of mass loss. The outcomes showed that up to 7.27% of mass loss, accelerated erosion utilizing the impressed strategy was compelling in initiating corrosion of concrete steel R/F. With respect to Faraday's law, the utilization of various current densities has no impact on the level of mass loss. Be that as it may, the expansion in the present thickness level above 200 mA/cm^2 leads to a noteworthy increment in deformation reaction and break width because of steel R/F corrosion. Therefore, it concludes that the impressed current is a dependable method for simulating corrosion of concrete steel R/F.

F.G. Baptista et al. [39] investigated the ideal size of PZT patches for structure wellbeing checking dependent on the EMI (Electromechanical Impedance) method. Hypothetical examination and test results fit well and show that the right PZT fix design can improve affectability to harm identification. Depending on the result, the fix must be little to guarantee low static limit and greater amplitude in the electrical pulse to ensure excellent results for the correlation coefficient deviation metric (CCDM) and root mean square deviation (RMSD) indices. In any case, if the mechanical impedance of the host construction is high according to the MI (Mechanical Impedance) of transducer, the increase in patch mark improves the affectability for harm location, especially when the correlation coefficient deviation metric index is utilized. It has been shown that an equal shipping system improves sensitivity and maintains a low static capacity. As referenced above, the planned method is appropriate for materials and structures with short damping where the cross-sectional series can be viewed as steady. Finally, the proposed method might be helpful for the correct size of PZT transducers, particularly in metal structures with short damping and strong mechanical impedance with respect to the MI of the transducer.

E. Nakamura et al. [40] reported that a practical program of potential scopes for corrosion evaluation on a present pre-tensioned concrete bridge close to the shore in Japan. According to experimental observations, they concluded that the most damaging potential area about the identical boundary map corresponds with this stage with higher chloride content and localized corrosion. They also concluded that the potential slope is a great indicator for choosing the place for additional destructive testing when there are not any indications of corrosion to the concrete surface. They also discovered that the measured potential merits fluctuated due to a number of things, such as fever, reference electrode kind, and pre-wetting moment. On the other hand, the potential gradient pattern stayed the exact same for its structure. Even the Equipotential Boundary chart is a much dependable instrument for discovering localizes corrosion and picking the place for additional destructive testing.

M. P. Ghaz et al. [41] modeled the potential dimensions supplied by resolving the Laplace's equation, even taking into consideration the impact of resistivity, pay depth, O_2 availability, and anode-to-cathode region (A/C) ratio over the potential mapping. Dependent on the outcome,

they concluded that at reduced resistivity solid and the potential distribution beside the outside carefully reflects the potential distribution in the border of steel/concrete. Since the resistivity of concrete increases, the potential distribution in the surface will part clearly from the steel/concrete interface. In accumulation, they discovered that using an increase in pay depth, the potential of this outside differed from the port considerably. They noticed that oxygen concentration from concrete isn't a substantial factor impacting potential dimension unless concrete is totally deprived of oxygen. A greater average potential value in the face of concrete suggests lower the likelihood of this corrosion according to ASTM (1999). On the other hand, the speed of this corrosion, if happening locally, has been discovered to be somewhat large. On the flip side, at small values of typical potential, the likelihood of this corrosion is greater, but this corrosion can go more closely. Precise detection of localized corrosion, where A/C ratio is modest, might not be achievable with potential dimension method unless additional measurements are created.

S. Bhalla et al. [42] introduced a new strategy to evaluate the fatigue length of bolted steel joints employing the equivalent stiffness depending on piezo- impedance transducers connected to the surface. The equivalent parameters of this plank were identified with the obtained electromechanical consumption signatures. During examining on three components metal joints, both empirical equations were made to link the whole period of staying fatigue into the equivalent identified reduction of stiffness. The most promising feature of this suggested approach is the fact that it directly applies the admittance of piezoelectric transducer signatures connected to the surface, thereby sustaining the conclusion of the in situ stiffness of the joint.

N. G. S. M. Rathod and N.C. Moharana [43] investigated that corrosion is the main cause of steel reinforcement degradation in concrete. Corrosion begins before cracks appear. This study discussed some non-destructive methods for detecting corrosion, as it isn't feasible to discover corrosion by visual ways. This record described several non-destructive techniques for tracking corrosion using different gear. From the Technique of Greater Surface Potential (SP), an electric current switch between the anodic & cathode websites in concrete through corrosion and can be sensed by measuring the potential reduction of concrete. The LPR (Linear Polarization Resistance) method just had a steel-reinforced link to quantify reinforced steel corrosion in

reinforced concrete structures. Potentio-dynamic anodic polarizations classify a metallic model via its own possible present relationship. These preceding methods were helpful simply to locate the place of the anode and cathode and didn't offer real-time confirmation outcomes. While to quantify real-time erosion approaches such as acoustic emission, galvanic observation probe, higher frequency UV transcends restriction.

S. Altoubat et al [44] investigation presented an experimental program to compare corrosion damage utilizing two quickened erosion strategies, specifically steady voltage and consistent current. Six concrete sections were tested in this study. A total of six reinforced deformed bars 13 mm in diameter and 6 millimeter in width winding were placed longitudinally. A 20-mm diameter stainless steel tube put in the middle of this pillar to work as a cathode. To accelerate erosion & to offer O_2 little gaps diameter of 2 millimeter and 4 no. were created across the steel pipe lengthwise. The exploration comprised of 2 components. The very initial segment let erosion approximately eight percent of steel reduction utilizing two approaches, consistent voltage, and constant current. The following part should rust the segments to your most extreme pressure load error. Findings bring there was an almost identical steel flow, but further damage was a result of a constant current. Because of this, serious structural damage to the constant current has diminished, as load capability has also diminished. As a result, the constant current approach generated more desirable results to provoke corrosion from the reinforced concrete part.

S. Bhalla and C. K. Soh [45] investigated that the two-section arrangement introduces a new simplified strategy for diagnosing structural harm with surface-related piezo impedance converters. The initial segment presents another model of elastic electro interaction, structured by PZT and dependent on the idea of "powerful impedance". The proposed plans can be utilized can be used correctly to remove, the mechanical impediment of an "obscure" structure system of the intake marks of a PZT fix stuck to the surface. This is an enhancement more accessible models, the intricacy of which restricts direct application in comparable down to earth situations. The second piece of this record will present a strategy for expelling the mechanical impedance from the structure through trial conductivity & suspension marks. It will likewise introduce a philosophy for evaluating structural harm utilizing the impedance spectra extricated from the

structure dependent on a proportional system approach. Notwithstanding non-destructive, the proposed model can be utilized in numerous different applications, for example, system reaction estimating, power change effectiveness, and system power utilization.

S. Bhalla and C. K. Soh [46] have discovered another system for structural ID (Identification) and non-destructive assessment by piezoelectric transducers. The initial part presented the hypothetical growth and investigational justification of the fundamental model of the PZT (Lead-Zirconium-Titanate) structure. In our recently proposed strategy, the harm assessed by the parameters of the proportional system is recognized" by the surface-bound piezo impractical transducer. As evidence of idea, the technique was successfully used to analyze damage to a delegate aerospace structure and a common structural prototype. It is then expanded to recognize and screen a model of a RC (Reinforced Concrete) scaffold throughout a damaging stress test. It was found that the proposed method was able to successfully identify and assess damage in both facilities. This document contains a few instances of recorded information on corrosion potential, electrical obstruction and erosion rates, as well as a approach for achieving a delegate rate of corrosion on average every year. The delegate worth can be utilized in predictive corrosion models to figure the rest of the lifetime.

S. Park and S. K Park [47] investigated wireless checking of erosion harm that can often happen in metal structures. For corrosion monitoring tests, a simple aluminum alloy beam structure was selected and a tiny PZT fix sensor for the structure was mounted on the surface. To get an EMI information system on the lead zirconate titanate sensor, a wireless sensor knob consisting of a scaled down estimating chip that prevents defects, microchip and RF telemetry was utilized. Figure 2.3 show the planned sensor node and its block figure.
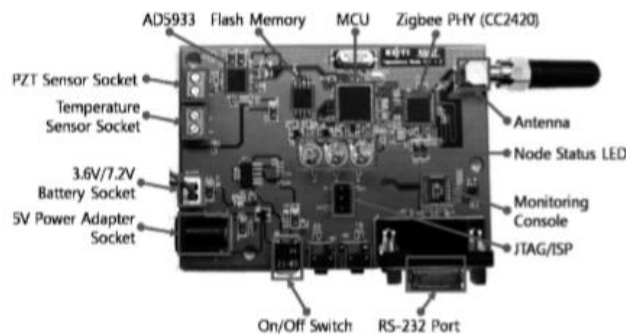
(a) Our impedance sensor node prototype
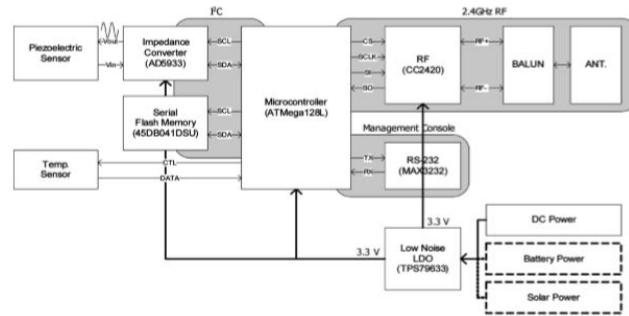
(b) Block figure

Figure 2.3: Wireless impedance sensor node (Source: S. Park and S. K Park [47])

Three distinctive consumption cases with another eroded surface were unnaturally added to the beam structure with hydrochloric acid (HCI) & electromechanical information were gathered sequentially by the radio protection sensor node. In order to evaluate the corroded range, changes in the resonance frequency, which represent dynamic structural information, were continuously monitored in all cases of damage. The EMI information was likewise gathered for every injury case (Figure 2.4).
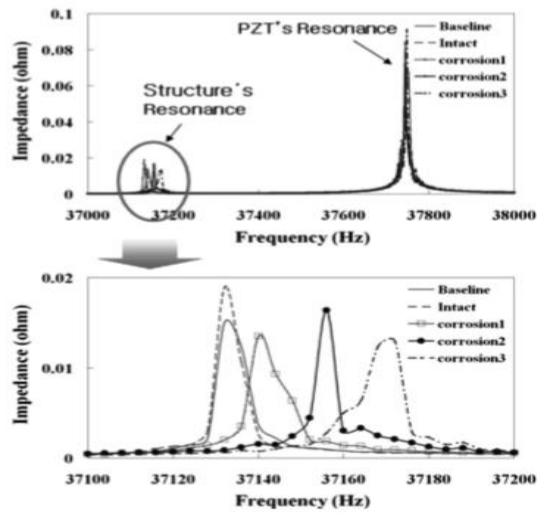

Figure 2.4: Difference of impedance mark because of corrosion damage (Source: S. Park and S. K Park [47])

30

Two kinds of resonance frequencies could be extricated: the first speaks dynamic structural data & second represent the dynamic information of the sensor. Conclusively, the amount of resonance frequency displacement increased as the corroded surface increased. The results showed that the proposed approach can be utilized adequately for the quantitative investigation of the eroded surface in metal structures utilizing the measure of resonance frequency shift to the calculated EMI.

M. Moreno et al [48] investigated that the impact of various levels of carbonation and the nearness of various chloride substance in reproduction arrangements was explored. The outcomes show the beneficial outcome of high alkalinity on the restricted erosion of steel brought about by chloride particles. The consequences of the potentio-dynamic tests assessed a basic chloride fixation for each solution over which the sting could take place. The chloride thresholds found here are in a similar request as those recently detailed in the writing for without film steel. The outcome of solutions simulating carbonated concrete demonstrated that non-passive carbon steel improved at low carbonation conditions, while localized corrosion resistance was improved at high carbonate and bicarbonate concentrations.

2.3 Research gaps

- Most of the literatures are concerned about corrosion detection in RCC structure using destructive method.
- There is lacuna in literature about real time corrosion monitoring of RCC structure.
- There are limited researches on the comparison and corrosion monitoring of different high-grade concretes.
- Limited literatures are available which provide use of electrical sensor for real time corrosion detection in RCC structures

2.4 Research objectives

- Real time corrosion monitoring of steel bars embedded with piezo-sensor by using EMI technique.

- To find out the compression test results of concrete cubes of different grades cured at different time span.
- To suggest the best suitable grade of concrete among three high grades this is less prone to corrosion.
- Comparative study of the compression test of concrete cubes and corrosion test results of concrete beams of Grades M40, M50 & M55.

CHAPTER 03
EXPERIMENTAL INVESTIGATIONS

3.1 General

Steel is utilized as reinforcement material in concrete structures because it's the best suited combination for concrete. Because of the reason that steel and concrete act to resist caused forces. The thermal expansion coefficients of steel and cement are all equivalent; yet, alongside a mind-blowing capacity to bond and twist with a solid body which makes steel exactly the reinforcement material in RC structures. One is steel corrosion, which can be just a problem detected with bases around the world. Recently, the enthusiasm of traditional researchers regarding the difficulty of corrosion of reinforcement bars has intensified because of the loss of foreign precious metals because of utilization, just as because of the deterioration of the basic characteristics. Corrosion of a steel stand has been distinguished as the most known reason for failure and early failure of RC structures.

This part introduces a new methodology with checking corrosion on exposed steel bars, utilizing the impedance-based procedure. By the surface-connected PZT patch the corrosion-induced damage is evaluated &depends on the equal parameters recognized. In these chapter specific experiments conducted refers to measure the electromechanical information.

In this chapter, the material used in conjunction with its properties and composition and the comprehensive experimental application and process was discussed. Originally, the important concrete properties were identified and the constraints of further cement substances were put. The properties of concrete that indirectly or directly impacted by some elements are discussed so that experimental arrangement could be made to examine the relative effect on concrete properties.

3.2 Research methodology

To achieve the research objectives that are explained in chapter 01, a successive methodology was suggested. The design of methodology is given in Figure 3.1.
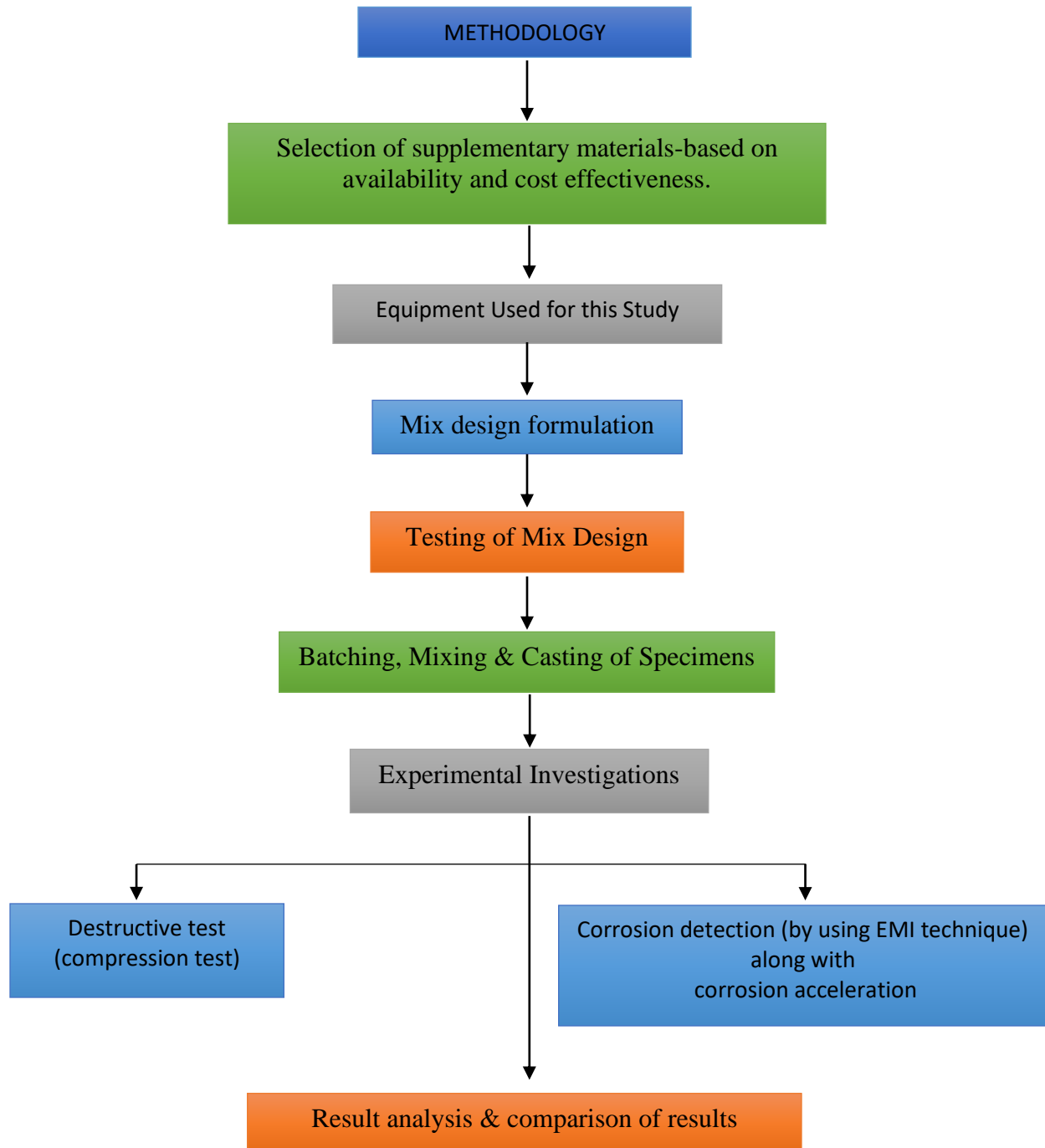
Figure 3.1: Layout of experimental methodology

Step 1: Materials selection

Subsequently through literature evaluation Ordinary Portland cement is used along with the superplasticizer was used for experimental investigation.

Step 2: Preparation of mix design

After the selection of material for mix design, individual mix design was prepared for different grades of concrete.

Step 3: Experimental study

(i) Compressive test
(ii) Corrosion detection test

(i) Destructive test:

Compression test was performed on the cube of size (as per IS codes). The comparison and results of different grades are tabulated in chapter 4.

(ii) Corrosion detection test:

For both the materials used corrosion acceleration was done by using NaCl solution. Along with corrosion acceleration corrosion monitoring was done by using PZT senor based on EMI technique. The comparison and results of different grades are tabulated in chapter 4.

Step 4: Results comparison

Corrosion result was examined by using electromechanical impedance technique. Instrument used to track the admittance values at different interval of time was oscilloscope. Different admittance values for both the materials at Specific interval of time was observed and compared with each other to find out the best suitable material from the both with is less prone to corrosion and will tends to perform better in actual scenario.

3.3 Material used

Fine and coarse aggregates are joined together to form a composite material called concrete, joined together with liquid concrete that hardens over time. Degree of compaction ensures the potential strength and quality of concrete of a given proportion of mixtures. In the attached sections the materials used for concrete planning are inspected.

3.3.1 Aggregates

Aggregates are one of the most important building materials, utilized as concrete and asphalt composite material, and as a base material in foundations, roads and railways. They provide volume, stability, wear or erosion resistance, and other desired physical properties to the finished product [49]. They also occupy around 75 percent of the volume of concrete and, therefore, their effect on different concrete properties is considerable.

Categorization of aggregate based on unit weight:

i. Aggregate of normal weight.
ii. Aggregate of light weight.
iii. Aggregate of heavy weight.

Table 3.1: Categorization of ordinary weight aggregates [49]

Natural aggregates	Artificial aggregates
Sand, Gravel, Crushed	Broken Brick
Rock such as Granite	Air-cooled Slag
Quartzite, Basalt	Sintered fly ash
Sandstone	Bloated clay

Classification based on size of aggregates:

1. Fine Aggregate
2. Coarse aggregate

The aggregate size larger than 4.75 mm is regarded as a rough aggregate and aggregate whose size is 4.75 mm and much less is treated as a fine aggregate. The form of the aggregates is a significant characteristic, as it impacts the workability of the concrete. It has a substantial role in the creation of high-strength concrete. Maximum size of around 40mm is employed for coarse aggregate in most structural uses.

Almost all-natural aggregates come in the bedrock. Out of those 3 igneous stones makes concrete exceptionally satisfying because they're typically difficult, tough and dense [50]. Both igneous rocks and sedimentary rocks may be determined by high pressures and temperatures which cause metamorphism that affects the structure and surface of stones. The arrangement, size and shape of the aggregate have an important effect on the functioning ability, durability, strength, weight and shrinkage of the concrete. The form of the aggregates is a significant characteristic, as it impacts the workability of the concrete.

Classification based on shape:

1. Rounded aggregate
2. Irregular aggregate
3. Angular aggregate
   (a) Flaky aggregate
   (b) Elongated aggregate

Surface texture is a property whose assessment relies upon the quantity of clean, smooth, or rough surfaces of the particles. The consistency of the surface depends upon the hardness, grain size, pore structure, rock structure and degree of smoothness or roughness of the forces following the particle limits. As surface perfection increases, the contact surface reductions, so a cleaned molecule will exclusively have a smaller surface area for adhesion to the matrix than a coarse molecule of a comparable volume. The physical properties of the aggregates utilized in this investigation are introduced in Tables 3.2 and 3.3.

For workable concrete, size distribution or grading of aggregate plays an important role. The size and shape of the aggregate affect the properties of new concrete more than simply hardened concrete. Concrete is more viable when round and smooth aggregate is used rather than rough angular or extended aggregate. Crushed stone generates more aerodynamic and more elongated

aggregates, which include a greater surface-to-volume ratio; greater bond attributes however need more concrete paste to produce a viable mixture. Arrangement of IS Sieve for its analysis is shown in Figure 3.2 [51].

Grading of coarse and fine aggregates are shown in Table 3.4 and Table 3.5 respectively. The grading limits for fine aggregate and coarse are clarified in IS 383-1970 [52]. For the study work, both CA and FA are purchased from locally available suppliers in Chandigarh. This is embedded in the mix ratio process. It is expressed as the sum of the collective %age of the engaged weight in a standard sieve-set divided by 100. Fineness modulus is used to determine the order of fine aggregates & is classified in Table 3.6.

Table 3.2: Physical properties: coarse aggregate (20mm size)

Sr. No.	Type of Test	IS Standard	Results
1	Water absorption	IS-2386-P-3	1.513%
2	Specific Gravity	IS-2386-P-3	2.75
3	Bulk density test	IS-2386-P-3	1436

Table 3.3: Physical properties of F.A. (Fine Aggregates)

Sr. No.	Type of Test	IS Standard	Results
1	Specific Gravity	IS-2386-P-3	2.67
2	Water absorption	IS-2386-P-3	7%

Table 3.4: Sieve analysis of C.A. (Coarse Aggregate)

IS Sieve Size (mm)	Weight of Aggregate Retained	% age of Total Weight Retained	Cumulative %age of Total Weight Retained	Cumulative %age Passing
Coarse Aggregate = 20mm				
Total Weight of Aggregate =1000g				
20	0	0	0	100%
16	47.3	4.73	4.73	95.27%
12.5	494	49.40	54.13	45.87%
10	347.7	37.47	91.60	8.40%
4.75	76.0	7.60	99.20	0.80%
pan	8.0	0.80	100%	Zero%

Table 3.4.1: Specification sieve analysis of C.A. (Coarse Aggregate)

IS Sieve Designation	Specification (IS-383:1970)					
	%age Passing For Single Size Aggregate of Nominal Size (mm)					
	63	40	20	16	12.5	10
80mm	100	-	-	-	-	-
63mm	85-100	100	-	-	-	-
40mm	0-30	85-100	100	-	-	-
20mm	0-5	0 - 20	85-100	100	-	-
16mm	-	-	-	85-100	100	-
12.5mm	-	-	-	-	85-100	100
10mm	0-5	0-5	0-20	0-30	0-45	85-100
4.75mm	-	-	0-5	0-5	0-10	0-20
2.36mm	-	-	-	-	-	0-5

Table 3.5: FA (Fine Aggregates) of sieve analysis

IS Sieve Size	Weight Retained	Cumulative Weight Retained	Cumulative %age Retained	Cumulative % age Passing	Zones I	Zones II	Zones III	Zones IV
	Total weight of fine aggregate = 1000gm				Specification (IS: 383-1970) Percentage Passing For			
10mm	0	0	0	100	100	100	100	100
4.75mm	13.3gm	13.3gm	13.3	99.86	90-100	90-100	90-100	95-100
2.36mm	49.1gm	62.4gm	62.4	99.38	60-95	75-100	85-100	95-100
1.18mm	118.4gm	180.8gm	1.80	98.2	30-70	55-90	75-100	90-100
600µ	91.7gm	272.5gm	2.72	97.28	15-34	35-59	60-79	80-100
300µ	174.7gm	446.2gm	44.6	55.4	20-5	30-8	12-40	15-50
150µ	453.7gm	901.1gm	90.1	9.9	0-10	0-10	0-10	0-15
Pan	98.9gm	1000gm	98.9	0				
Total	1000gm	Fineness modulus = 2.46						

Figure 3.2: Analysis of sieve

Table 3.6: Fine aggregates on the basis of fineness modulus (F.M.) [50]

Fine	F.M.	2.3-2.6
Medium	F.M.	2.6-2.9
Coarse	F.M.	2.9-3.2

3.3.2 Binder

Ordinary Portland cement (OPC)

Cement can be categorized as the cohesive & adhesive properties of bonding material which permits us to join the different building materials. The most generally utilized types of Portland cement is normal Portland cement. Lime, silica, alumina and iron oxide are the main raw materials utilized for cement production. The cement creation process consists of crushing the raw materials, carefully blending them in certain proportions according to their composition and purity, and processing them in a furnace at a temperature somewhere in the range of 1300 and 1500°C, to which the sintered material is formed and, to some extent, fused to form a nodal clinker. The clinker is cooled and milled into fine powder with the accumulation of 3 to 5% gypsum. One component formed by this technique is Portland concrete. Tri-calcium silicate and dialcium silicate are the most significant quality blends.

Figure 3.3: Ordinary Portland cement

The ordinary Portland cement (OPC) has categorized by the bureau of Indian standards (BIS) to three levels so as to create different grades of concrete to fulfill the requirements of the building businesses. This sorting was depending on the 28-day compression force as follows:

1. OPC of Grade 33– IS 269: 1989
2. OPC of Grade 43– IS 8112: 1989
3. OPC of Grade 53– IS 12269: 1987

Ordinary Portland Cement (OPC) of Grade 43 from single source (Ambuja Cement) is used throughout the research work. The cement properties in current project compliant to IS 8112-1989 are presented below in Table 3.7 [54-53]. OPC 43 grade was purchased by Ltd Darlaghat. Figure 3.3 shows OPC cement.

Table 3.7: Physical properties: Ordinary Portland cement

Property	Average Value	Standard Value as per IS 8112-1989
Specific gravity	3.129	
Normal Consistency	32%	
Initial setting time	40	>30min
Final setting time	460	<600min
Fineness	5% retained	
Compressive Strength		
3-days	24 N/mm^2	>23
7-days	35N/mm^2	>33
28-days	46N/mm^2	>43

3.3.3 Water

Water plays an extremely huge function in the concrete-mix. There are following two main reasons which signifies it's need:

Bonding: Mixing of cement with other ingredients of concrete with water as a binder. And also, to produce unique structures, water can also be responsible for the practice of hydration that contributes to the hardening of concrete.

Workability: This really is the simplicity of mixing concrete. Additionally, it may be considered the fluidity of the concrete. As a result of Water, concrete could be readily blended to make the desired mix. The function of water is to decrease external friction between the concrete and all those gears used to combine it. It Is due to the workability eased by water which concrete could be moulded into different shapes before it may harden.

For concrete production use of water also depends on the pH value of water. PH in between 6 to 8 is free from organic compound. Water-concrete ratio ensures the strength of concrete. Cement gel hydration is shown in Figure 3.4 with the given ratio of (w/c 0.2, 0.3 and 0.5). A small amount of water can be used to hydrate the cement and to lubricate the mixture extra water is required. Some capillary pores could be formed due to the excess of water& strength of concrete could decrease with excess use of water [49].
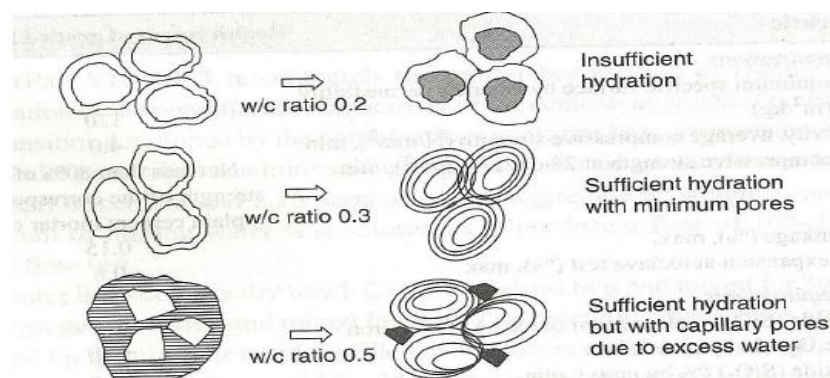
.

Figure 3.4: Presentation of hydration based on amount of water [49]

3.3.4 Superplasticizers (High Range Water Reducers)

Superplasticizers are a reasonably new class and a better variant of the plasticizer, the utilization of that was made in 1960 and 1970 respectively in Japan and Germany. They are chemically distinct from ordinary plasticizers. The utilization of superplasticizer reduces water by around 30 percent without diminishing functioning capability, when compared with a reduction of around 15 percent for plasticizers. This raises the workability at a specified w/c ratio, generally increasing the slump from 75 mm to 200mm. The principal issue is these superplasticizers is as strong as a dispersant and therefore are high-end water reducers. They're known as High Range Water Reducers in American literature. It's the potential of superplasticizer which has allowed to use w/c as low as 0.25 or lower and to create flowing concrete to find the strength of this sequence 120 MPa or more. The properties of superplasticizer were referenced in the IS: 9103-1999 [55].

3.3.5 Equipment utilized

a) Piezo -electric Sensor

The word 'piezo' originates from Greek words that mean pressure. The phenomenon of piezoelectricity was found in 1880 by Pierre and Paul-Jacques Curie. It is found in balanced non-central crystals, such as quartz (SiO_2), Liithium Niobate ($LiNbO_3$) and lead zirconate titanated [PZT, Pb ($Zr1-xTix$) O_3], where electric dipoles (surface charges) is generated when the crystal is exposed to mechanical stress [57].Piezoelectric materials have an exceptional property of producing electrical dipoles (reverse surface fees) when subjected to mechanical pressure (see Figure. 3.5 a) and they endure mechanical deformations when subjected to electrical fields as revealed in Figure 3.5 (b).

A piezoelectric sensor is a device that utilizes the piezoelectric effect, to quantify changes in pressure, acceleration, temperature, stress or force by changing them into an electric charge. The piezoelectric material as a PZT patch is probably the best material for structural health monitoring (SHM) and damage detection in the civil, mechanical and aerospace installations [56]. Apart from its unique properties, its low cost, size and easy installation have been the key factors for being most preferred material for continuous monitoring of engineering amenities.
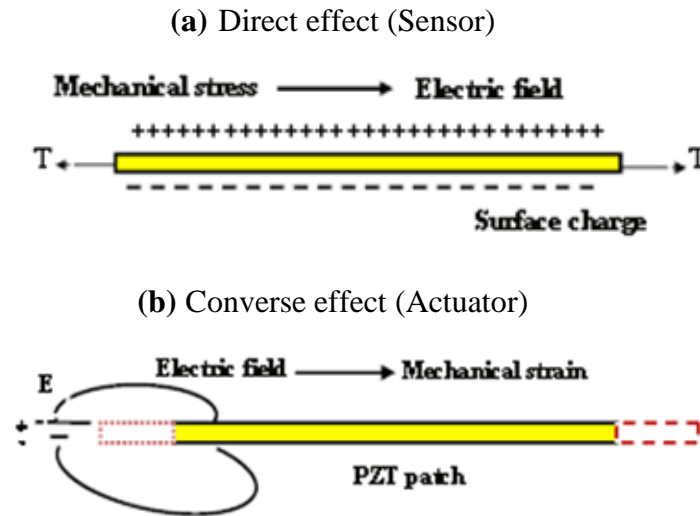
(a) Direct effect (Sensor)

Mechanical stress   ⟶   Electric field

++++++++++++++++++++++++++++++++

T ◂——[⬜⬜⬜⬜⬜⬜⬜⬜⬜⬜⬜⬜⬜⬜⬜⬜⬜⬜]——▸ T

– – – – – – – – – – – – – – – – –

Surface charge

(b) Converse effect (Actuator)

Electric field ⟶ Mechanical strain

E

PZT patch

Figure 3.5: Direct and converse effect of piezoelectric materials [56]

Different kinds of PZT patches are accessible on the market in various shapes for example, round, rectangular, square and different sizes. Characteristic of this patch is the electrode of the lower edge is wrapped across the depth, so both electrodes are available on a single side of the PZT patch, whereas the other hand is readily secured to the host structure.
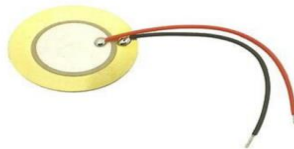
Figure 3.6: Lead Zirconate Titanate-Piezoelectric ceramic sensor

The PZT round sensor is used in this project for structural health monitoring. The lead zirconate titanate piezoelectric ceramic sensor is use in this project for structural health monitoring (as shown in Figure 3.6). A set of sensors was ordered using online internet platform (amazon.in website).These are 27mm diameter gold color Piezo Discs made by Prielsys Enterprises.

b) Oscilloscope

An oscilloscope is a device for measuring electronic signals and is found in several scientific laboratories (as shown in Figure 3.7). It is operated to watch variable sign voltages on a two-

dimensional system that represents time [57]. When the oscilloscope is connected to an energy source via a probe, it immediately displays the corresponding waveform in real time. Although they are mainly used in science and technology, they are also used in other areas such as telecommunications and medicine.
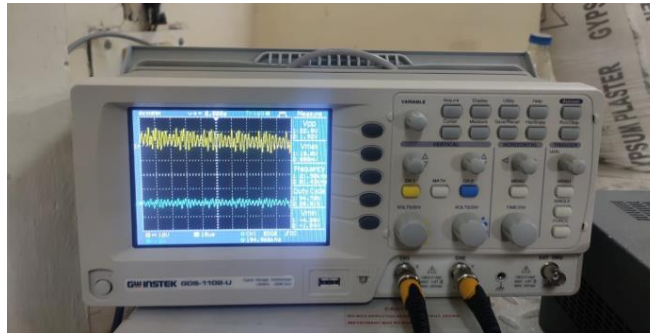

Figure 3.7: Oscilloscope

There are different types of digital and analog oscilloscopes, and the variations of oscilloscope are as follows:

- Analog sampling oscilloscopes
- Hand-held oscilloscopes
- Computer-based oscilloscopes
- Mixed-signal oscilloscope

The difference in constraints like sample speed, memory thickness, number of channels, probe demand, bandwidth, along with analytic capacity to determine that oscilloscope is most suitable for a specific atmosphere. Oscilloscopes can gauge the frequency and amplitude of a signal and signal the form of the shaped sign. Additionally, it supplies all qualitative and qualitative details concerning the time period, ascent period and distortion of this shaped sign. But as they're primarily made for the monitoring of waveforms, oscilloscopes are somewhat less precise than other evaluation devices for measuring direct current voltages.

3.4 Mix design

In concrete mix design cement sand and aggregate are mixed in accurate proportion to achieve desired strength. The concrete mix design entails various measures, calculations and lab testing

to discover appropriate mix proportions. This process is usually adopted for structures that require higher levels of concrete like the M25 and over and big construction jobs where the quantity of concrete ingestion is enormous. An advantage of concrete mix design is that it supplies the ideal proportions of substances, thus creating the concrete construction cheap in attaining required power of structural members. As, the number of concrete necessary for big constructions are tremendous, economy in volume of materials like cement makes the job construction cheap. Mixed design can be characterized as the best approach to pick reasonable concrete components [49]. The inspiration behind the planning, as found in the definitions above, is two-fold. The fundamental objective is to accomplish the lowest durability & strength.

Developing of concrete is the second objective. All concretes that are noticeable depend mainly on two variables; equipment-specific costs and labour costs. For a good concrete, the labour costs of formworks, bunching, mixing, transport and hardening are almost. The expense of the various elements is less than the cost of concrete; the emphasis is on utilizing less concrete, if necessary, compatible with quality and durability. From this point of view, the main consideration is the expenditure of materials [58].

Specifications and data used for Mix proportioning for concrete of M40, M50 and M55 grade are accounted below:

a) *Mix proportioning for a concrete of M40 grade***:**
  1. Design Specifications [59]
    a) Designation of grade = M40
    b) Cement used = OPC 43grade (IS 8112: 1989)
    c) Aggregate Size (Max.) = Below 20mm angular
    d) Supervision Mark = Good
    e) Exposure condition = Severe (meant for reinforced concrete)
  2. Test data for materials
    a) Cement used = OPC 43grade (IS 8112:1989)
    b) SG of cement = 3.129
    c) SG of CA = 2.75
    d) SG of FA = 2.67

e) Water absorption of CA =1.513%

Table 3.8: Mix design proportions of M40

Water to cement ratio : 0.45			
Water	Cement	Fine aggregate	Coarse aggregate
190kg/m^3	399kg/m^3	632kg/m^3	1129kg/m^3

Final mix design – 1:1.58:2.8

b) Mix proportioning for a concrete of M50 grade:

1. Design Specifications

   a) Designation of grade = M50

   b) Cement used = OPC 43grade (IS 8112: 1989)

   c) Aggregate Size (Max.) = Below 20mm angular

   d) Supervision Mark = Good

   e) Exposure condition = Severe (meant for reinforced concrete)

2. Test data for materials

   a) Cement used = OPC 43grade (IS 8112:1989)

   b) SG of cement = 3.129

   c) Chemical admixture = superplasticizer

   d) SG of CA = 2.75

   e) SG of CA = 2.67

   f) Water absorption of CA =1.513%

Table 3.9: Mix design proportions of M50

Water to cement ratio : 0.35			
Water	Cement	Fine aggregate	Coarse aggregate
190kg/m^3	399kg/m^3	632kg/m^3	1129kg/m^3

Final mix design – 1:1.58:2.8

c) Mix proportioning for a concrete of M55 grade:

1. Design Specifications

    a) Designation of grade = M55

    b) Cement used = OPC 43grade (IS 8112:1989)

    c) Aggregate Size (Max.) = Below 20mm angular

    d) Supervision Mark = Good

    e) Type of exposure condition = Severe (meant for reinforced concrete)

2. Test data for materials

    a) Cement used = OPC 43grade (IS 8112:1989)

    b) SG of cement = 3.129

    c) Chemical admixture = Superplasticizer

    d) SG of CA = 2.75

    e) SG of FA = 2.67

    f) Water absorption of CA =1.513%

Table 3.10: Mix design proportions of M55

Water to cement ratio : 0.32			
Water	Cement	Fine aggregate	Coarse aggregate
143.8kg/m^3	410.85kg/m^3	752kg/m^3	1227.38kg/m^3

Final mix design – 1:1.83:2

3.5 Material's testing

3.5.1 OPC Cement

a) Normal Consistency

It's defined as the percentage of water from weight of cement that generates a consistency that lets a plunger of 10mm diameter to penetrate to a thickness of 5mm to 7mm over the base of vicat's mold. The Vicat device was utilized from IS: 4031 Part 4:1988 [60]. In OPC cement the normal consistency is 35.5%.

Figure 3.8: Normal consistency

b) Initial setting time

First setting time of cement would be your lapse between the inclusions of water along with the instantaneous cement paste begins to shed its plasticity without sacrificing its potency. It's the period when water has been added to the cement and also the time in that needle of $1mm^2$ segments neglects to penetrate the thickness of the block into a thickness of 5to 7mm in the Vicat mold. The IST is 40 minutes.

c) Final setting time

Final setting time is the time lapse between the addition of water to the instant the cement paste completely loses its plasticity. It is the time when water is added to the cement and the time when the 1 mm needle establishes an impression on the dough in mold, however the 5mm accessory doesn't make an impression. The FST is 460 minutes.

d) Specific gravity

Specific gravity, also referred to as relative density, is that the portion of the density of a substance to the density of a reference substance; equates with the portion of the mass of a substance into the mass using a reference substance for the same specified quantity. The apparent specific gravity is the ratio of the burden of some of this substance to the weight of an

equivalent quantity of the reference substance. The density jar procedure is used for calculating the specific gravity of this cement.

Figure 3.9: Specific gravity of cement

We have used water to calculate the specific gravity of this substance. However, we used kerosene in cement to come across gravity. This is only because cement is sterile and creates calcium when answered with water. The cement indicates no response when mixed with kerosene. In lab SG is 3.129 (see Figure 3.9).

e) Compressive strength

In the mortar cubes, folding resistance of the cement is considered by a compression resistance. For cement mortar production normal sand is utilized. Compression test machine was utilized for compression tests with cube volume70.6mm^3.

Figure 3.10: Cubes preparation for compression test

Results of compressive strength (CS) are:

- After 3 days of curing(CS) – 24 N/mm^2
- After 7 days of curing(CS)– 35 N/mm^2
- After 28 days of curing(CS)– 46 N/mm^2

3.5.2 Sand

a) Specific gravity (SG)

Density bottle dictated the specific gravity of sand. Sand particles made out of quartz have a SG from 2.65 to 2.80. Weights are given below

Empty bottle (W1) = 694gm

Bottle + sand (W2) =850.2gm

Bottle + sand + water (W3) =1551.1gm

Bottle + water (W4) = 1420.2gm

SG of sand =W2 – W1÷ (W4 –W1) – (W3 – W4)

SG of sand using density bottle = 2.67

3.5.3   Coarse Aggregates

a) Water absorption

In the concrete mixture, coarse aggregate tends to absorb water. Incomplete hydration of the cement may occur if there is decrease in water content& if not taken into account. From range 0.1-2.0% water absorption takes place. In research facility tests, the absorption of water from coarse aggregates is 1.513%

Absorption of water = $\frac{(A-B)}{B} \times 100$

b) SG (Specific gravity)

From the outcome of the water absorption test the specific gravity of the aggregates was considered as follows:

Weight of,

Saturated Aggregate (SA) on hold with container in water (W1) = 1.75kg

Container suspended in water (W2) = 0.49kg

SSD (saturated surface dry) aggregate in air (W3) = 1.955kg

OD (oven dried) aggregate = 1.925kg

SG of aggregates = 2.75

3.6 OPC specimens: casting, mixing & batching

To conduct the experiments, High yield deformed (HYD) steel bars of gradeFe415 (IS:1786, 1985) of 450 mm length and different diameters of 8mm, 12mm and 16 mm were selected. To get a smooth surface in the middle section all bars were machined to bond the patch (see Fig. 3.11). A thin layer of two-piece epoxy adhesive was applied to the machined surface and 27mm diameter PZT patch and grade PIC 151 (PI Ceramics, 2012) were applied (see Figure 3.12). A small weight is used to apply light pressure over the complete surface. To allow the complete curing of bonded material, complete setup was left intact at room temperature for 1 day. For the determination of corrosion test, concrete specimens were prepared by using rectangular moulds of size (100mm x 100mm x150mm). And also, to measure the compressive strength of concrete cubical moulds of size 150mm x 150mm x 150mm were prepared. The preparation of moulds is shown in Figure 3.13. All specimens are ready in according to the Indian Standard Specifications IS: 516-1959 [62]. A total of 27cubes and 9beams are prepared. In this experiment we provide clear cover of 45 mm. For the entire process Ordinary Portland cement of grade-43 from single source was used. After preparing the concrete of the cement, sand and aggregate mixture (as shown in Figure 3.14), three mixture designs M40, M50, M55 were used to cast a total of 9 beams (3 of M40, 3 of M50 and 3 of M55) and 27 cubes (9 of M40, 9 of M50 and 9 M55). Admixture was only used for the M50 and M55 design. Steel rebar of diameter 12mm, 16mm, 20mm with concrete of M40 grade were used, samples were designated as OX_1, OX_2, OX_3 and with M50 grade is also prepared with similar diameter size sand samples were designated as OY_1, OY_2, OY_3. Also, with M55 grade and samples were designated as OZ_1, OZ_2 and OZ_3. Specimens of different grades are shown in Table 3.11. In the reinforcing projecting side, a wooden end of size (100 mm x100mm) was utilized to provide backing. Before starting the casting process, all molds were oiled after cleaning properly. Specific consideration was reduced for keeping the oil from penetrating the reinforcing steel, because this might be injurious to the force of this ray due to the lack of durability of this joint which wouldn't be identified into years of corrosion. Predicated on the reinforced spans got, the most bizarre surfaces were selected to use from the tests

Figure 3.11: Rebar specimen prepared For bonding

Figure 3.12: PZT on surface of rebars

Figure 3.13: Mould preparation

Figure 3.14: Preparation of concrete mix

Figure 3.15: Samples Casted

Figure 3.16: Cured Samples

All these are rigorously substituted to fix the size prior casting. Consideration was paid into the molds in order there are not any spaces left at which there's a prospect of plastic concrete blockage. Careful strategies are embraced in batch processing, mixing and casting surgeries (Figure 3.15). From there forward, rough aggregates were inserted. Subsequently the water along with superplasticizer was carefully inserted so no liquid was leaking throughout the mix. The concrete mix was prepared by the cement mixer and also with manual blending. It was initially cleaned out of the water and following that dried to ensure that impurities do not stick to the surface from before usage. All samples were abandoned in the steel mould for the initial 24 hours beneath ecological conditions. From there forward, they had been closely de-moulded from the aging requirement so that no borders have been broken &established in the aging tank in room temperature for aging was 27 ± 20 as per IS: 10262-1982 (Figure 3.16) [59]. Concrete should be suitably considered to develop its perfect properties. The illustrations have been immediately immersed into the water to prevent water from evaporating out of hydrated concrete

Table 3.11: Specimen categorization

Grade	Specimen Name	Dia. of Steel Bar (mm)	Cover Depth(mm)
M40	OX_1	8	45
M40	OX_2	12	45
M40	OX_3	16	45
M50	OY_1	8	45
M50	OY_2	12	45
M50	OY_3	16	45
M55	OZ_1	8	45
M55	OZ_2	12	45
M55	OZ_3	16	45

3.7 Impressed current technique

Impressed current technique is used to accelerate the corrosion of reinforcing steel. The current technique, moreover referred to as a galvanostatic technique, in which Dc power source is

utilized to supply constant current flow to steel embedded into the concrete to organize to cause substantial corrosion in a quick moment. After employing the current for a certain period of time, the amount of induced corrosion may be determined by the law of electromagnetism, or the percentage of the actual amount of steel dropped in corrosion could be determined with the Aid of a gravimetric test conducted on the bars extracted resulting accelerated corrosion [65].

Impressed current technique to accelerate corrosion by using Set-Ups

In impressed current technique devices used are electrode, electrolyte and a DC power supply. Steel rod is connected with the positive terminal behaves as anode and counter electrode was attached with negative terminal behaves as cathode. Cathode and anode both were attached with DC power supply (see Figure 3.17).
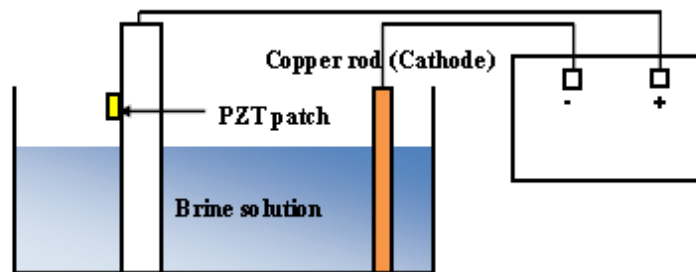

Figure 3.17: Accelerating corrosion setup [65]

The current is impressed by the counter electrotroding of the reinforcement by the concrete with the electrolyte (usually the sodium chloride solution). To get a desirable outcome within less time period, impressed current technique to accelerate the corrosion was conducted. In this study we utilized 3.5% NaCl solution.

.

CHAPTER 04
RESULTS & DISCUSSION

4.1 General

In this chapter, final outcomes of the compression test and accelerated corrosion tests carried out concrete cubes and beams. After that corrosion test results of concrete beams of all three grades (M40, M50, M55) was compared. The evaluation of corrosion has been done with the PZT patches bonded on the surface of particular rebars, using the impedance technique. The corrosion evaluation models are developed based on the analyzed data. While all of the previous research has concentrated upon metal parts plus employed the raw conductance signature with regard to corrosion monitoring as discussed in chapter 2, the research covered in this chapter focuses on corrosion in RC constructions utilizing the equivalent structural parameters extracted through the mechanical impedance, after filtering away the PZT guidelines. The next part of the chapter works with the comprehensive experimental study, data acquisition, analysis, plus the progress of the corrosion assessment model dependent on the comparative parameters.

Also, this chapter presents all of the compression test outcomes on the 27 concrete cubes of three grades (i.e., M40, M50, M55). Experimental results of a new corrosion measurement approach with regard to bare steel bars using the EMI technique through the use of the application of surface-bonded PZT patches based on the extracted structural parameters from the impedance spectrum. This chapter extends the suggested method to the rebars embedded inside the concrete and presents corrosion assessment comparison versions that can work extremely well in real-life corrosion monitoring of structures.

4.2 Tests conducted

To check the compression strength CTM (Compression Testing Machine) and for corrosion detection EMI technique were used. Final results of both the tests are accounted in this chapter.

4.2.1 Compressive strength test.

4.2.2 Corrosion Detection test.

4.2.1 Compressive strength test

Proportioning of concrete is used to control the strength of concrete, rough and fine aggregates, water, and assorted admixtures. To determining power of concrete, proportion of the water into cement is the main factor. The compressive strength is more when there is low water-cement ratio is used. The capacity of concrete is currently stated as MPa - mega pascals in SI units and psi - lbs per sq. inch in US units. This is usually caused due to the compressive strength characteristic of real fc/fck. Concrete having strength strength ranges from 10 MPa to 60 MPa can be ideal for normal field applications For certain applications & designs high compressive strengths concrete in the range of 500 MPa, are produced, commonly referred to as ultra-high strength concrete or chemically active concrete powder.

Figure 4.1: Compression testing machine

On hardened concrete, compression evaluation is the most common test that could be conducted, partially as it is a simple test to do, and compressive strength test can provide more practical usable properties of concrete. The compressive strength of concrete is given concerning the characteristic compressive strength of 150-millimeter size cubes tested at 28 days (fck) (as shown in Figure 4.1). The strength of concrete must figure out the strength of their members. Concrete specimens have been casted and analyzed under the act of compressive loads to ascertain the strength of concrete [62].

Within this study work concrete with quality control was prepared under restrained exposure state. To avoid any effect on the compressive strength, they are poured into cubical molds and put on a table to lessen air entrapped inside the molds. Removed of molds after1 day the molds the specimens were retained for healing at room temperature before testing. For the Compressive evaluation, we've ready 9 cubes of every grade. i.e., total 27 cubes were tested (as shown in Figure 4.2).


Figure 4.2: Concrete cubes of different grades used for compression test

For the purpose of compressive strength, these specimens were analyzed at several ages i.e., they are cured for 7 days, 14 days and 28 days. The load of roughly 140 kg/sq cm/min has been implemented without any jolt and load was improved continuously at a speed of before rising load breaks it down, without an increased load could be sustained. We noted down the maximum load applied to the specimen. The equal strength of this specimen was calculated by dividing the maximum load by tile region of contact of the bearing plates and has been stated to the nearest kg/sq cm. Typical of 3 values is accepted as the agent of this batch supplied the individual variation isn't greater than $\pm$ 15% of their typical. If not, replicate evaluations are taken.

For every grade, 3-3 cubes were divided into three batches (i.e., Batch1, Batch2 & Batch3). For M40 grade, total 9 cubes were divided into three batches designated as $C40_1$, $C40_2$, $C40_3$, $C40_4$, $C40_5$, $C40_6$, $C40_7$, $C40_8$ and $C40_9$.
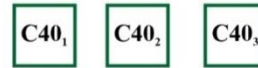
For Grade M40, compression test results of batch 1 were taken after 7 Days of curing. Which have the minimum average compressive strength of 28.69 Mpa. Cubes of Batch 2 were cured for 14 days. Average compressive strength of batch 2 was 42.57 Mpa. Maximum compressive strength of 46.83 Mpa was obtained after 28 days of curing for batch 3. Compression test results of M40 are given in following Table 4.1.

Table 4.1: Compressive strength (N/mm^2) of Grade-M40

Batch 1			Batch 2			Batch 3		
Day 7			Day 14			Day 28		
Compressive Strength (MPa)								
$C40_1$	$C40_2$	$C40_3$	$C40_4$	$C40_5$	$C40_6$	$C40_7$	$C40_8$	$C40_9$
28.10	29.89	28.10	42.89	42.41	42.41	46.34	46.34	47.89
Average compressive Strength(MPa)								
28.69			42.57			46.83		

For M50 grade, 3-3 cubes were divided into three batches (Batch1, Batch2 & Batch3) designated as $C50_1$, $C50_2$, $C50_3$, $C50_4$, $C50_5$, $C50_6$, $C50_7$, $C50_8$, $C50_9$.

For Grade M50, compression test results of batch 1 were taken after 7 Days of curing. Which have the minimum average compressive strength of 36.63 Mpa. Cubes of Batch 2 were cured for 14 days. Average compressive strength of batch 2 was 49.97 Mpa. Maximum compressive strength of 54.383 Mpa was obtained after 28 days of curing for batch 3. A compression test result of M50 is given in following Table 4.2.

Table 4.2: Compressive strength (N/mm^2) of Grade-M50

Batch 1			Batch 2			Batch 3		
Day 7			Day 14			Day 28		
Compressive strength(MPa)								
C50$_1$	C50$_2$	C50$_3$	C50$_4$	C50$_5$	C50$_6$	C50$_7$	C50$_8$	C50$_9$
36.40	36.40	37.10	50.64	48.63	50.64	52.76	52.76	57.63
Average compressive Strength(MPa)								
36.63			49.97			54.383		

For M55 grade, 3-3 cubes were divided into three batches (Batch1, Batch2 & Batch3) designated as $C55_1$, $C55_2$, $C55_3$, $C55_4$, $C55_5$, $C55_6$, $C55_7$, $C55_8$, $C55_9$. A compression test result of M55 is given in following Table 4.3.

For Grade M55, compression test results of batch 1 were taken after 7 Days of curing. Which have the minimum average compressive strength of 39.16 Mpa. Cubes of Batch 2 were cured for 14 days. Average compressive strength of batch 2 was 54.49 Mpa. Maximum compressive strength of 58.57 Mpa was obtained after 28 days of curing for batch 3. A compression test result of M50 is given in following Table 4.3.

Table 4.3: Compressive strength (N/mm^2) of Grade-M55

Batch 1			Batch 2			Batch 3		
Day 7			Day 14			Day 28		
Compressive strength (MPa)								
$C55_1$	$C55_2$	$C55_3$	$C55_4$	$C55_5$	$C55_6$	$C55_7$	$C55_8$	$C55_9$
40.01	38.73	38.75	53.45	55.02	55.02	57.13	57.13	61.45
Average compressive Strength(MPa)								
39.16			54.49			58.57		

Batch1, Batch2 & Batch3 of all three grades were tested after 7 days, 14 days and 28 days. Averages of every batch of all three grades were taken for research reference. The compression test results are tabulated in the above tables. We get maximum average compressive strength of 58.57Mpa for grade M55 which is cured for 28 days, followed by average Compressive strength of 54.383 Mpa for grade M50 and 46.83 Mpa for grade M40 both were also cured for 28 Days.

4.2.2 Corrosion detection test

a) Mechanism of the corrosion detection method

It is known that different types of oxidation products are formed during corrosion process. Due to the different material properties of corrosion products, volume of corroded part of a steel bar may increase. The Ultrasonic wave are guided through the steel bar as they are designed to do so. The wave energy would transmit to the part of concrete when the sensor was embedded into concrete [57]. Less wave energy would release to the concrete when the corrosion products were gathered. Thus, wave amplitude would change during the corrosion. The working principle is shown in Figure 4.3.
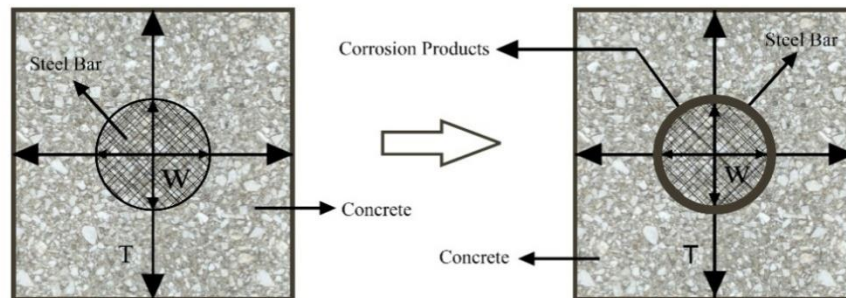

Figure 4.3: Propagation of ultrasonic waves in steel bar and concrete

(W: wave propagating in steel bar)

(T: wave transmitted into concrete) **[57]**

4.3 Experimental setup

The piezo sensor bonded with the concrete specimen was placed in the solution of 5% NaCl. The DC power has been connected with the corrosion circuit. The anode was connected with embedded reinforcement bar and cathode was connected with the copper rod of their direct-

current power. Both ends of metal rods were connected using a oscilloscope and signal generator (as shown in given Figure 4.4).
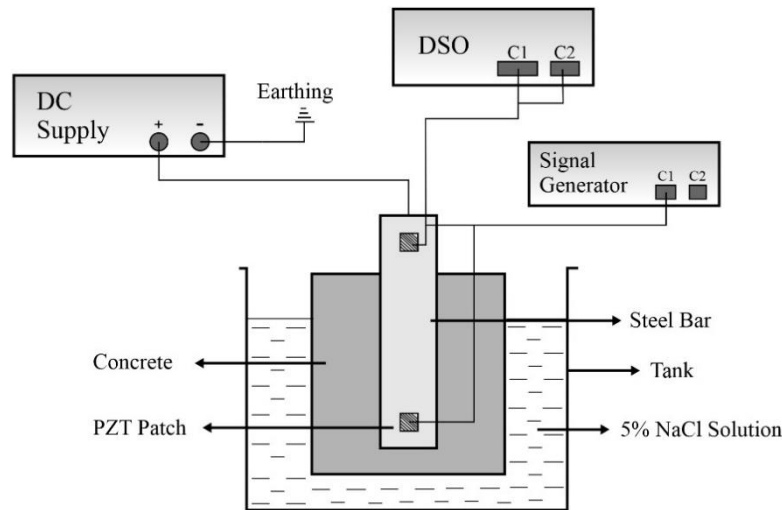

Figure 4.4: Corrosion monitoring setup

An electric pulse from a signal generator (SFG 1030) was stimulated with one piezoelectric component by along with another piezoelectric element. And this was utilized to get the ultrasonic wave that had been captured by an oscilloscope (GDS-1102-U). The input pulse was a step function of ±10V. Using a cover depth of 10 mm, sensor was then casted into the concrete beam. Wave amplitude was listed for all of the concrete grades. It may be noticed that the detector could respond to the changes in its surrounding. Then, to track corrosion monitoring the utilized sensor was shown in Figure 4.5.

Figure 4.5: Test instruments used in corrosion monitoring

The 5 volts of potential was used in the acceleration test. The ultrasonic wave signals were measured at particular interval of time. The amplitude of wave detects the initiation of the corrosion in the OPC concrete beam.

We have taken total 3-3 concrete beams of all three grades i.e., M40, M50 and M55. So total 9 concrete beams were monitored. Ultrasonic waves were recorded at 10hr, 30hr and 50hr for all three grades. During the initiation period the wave signals first measured at 10h were shown in the Figure 4.6.
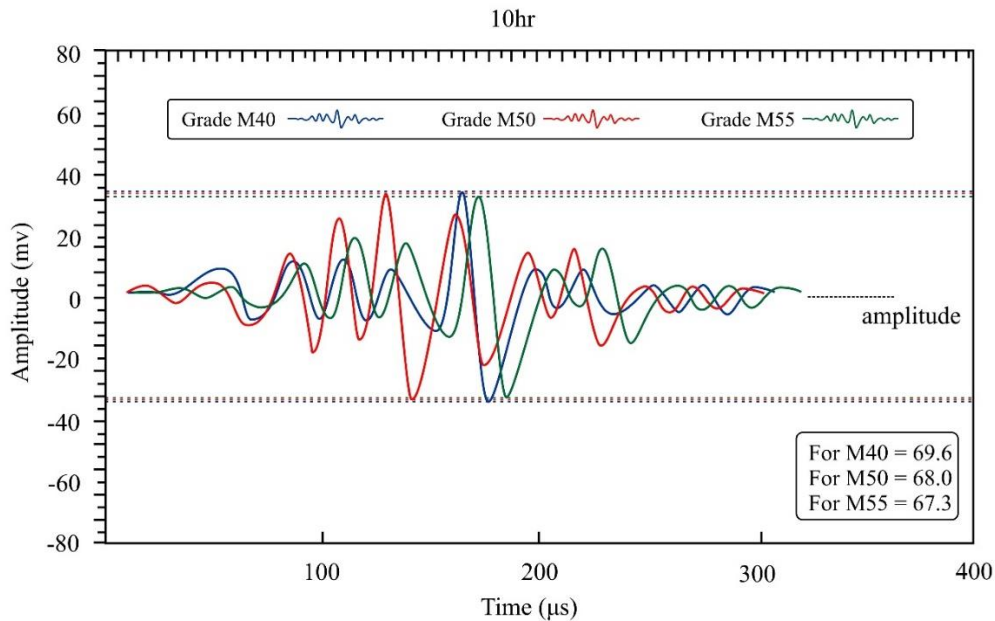

Figure 4.6: Ultrasonic waves recorded at 10hr

During initiation of corrosion monitoring test amplitude was started recording at 10hr, maximum amplitude 69.6 was recorded for grade M40 and minimum amplitude of 67.3 was recorded for grade M55. Amplitude on M50 was 68.0. The initiation of corrosion was first started on grade M40 later on M50 & M55. Thus, Grade M40 shows maximum deflection during starting hours of examination.

Initially, there was small deflection in the recorded wave, but through corrosion that the amplitude of the wave improved. The motive was it improved since with the increase in the corrosion period, the amplitude of the frequency peak declines gradually. Since the corrosion product layer decreases the transmitted wave energy and of those new appeared peaks rises.

Therefore, amplitude increases. The next values of amplitude were taken after a gap of 20-20hr. The waves recorded at 30hr and 50hr are shown in the Figure 4.7 and Figure 4.8.
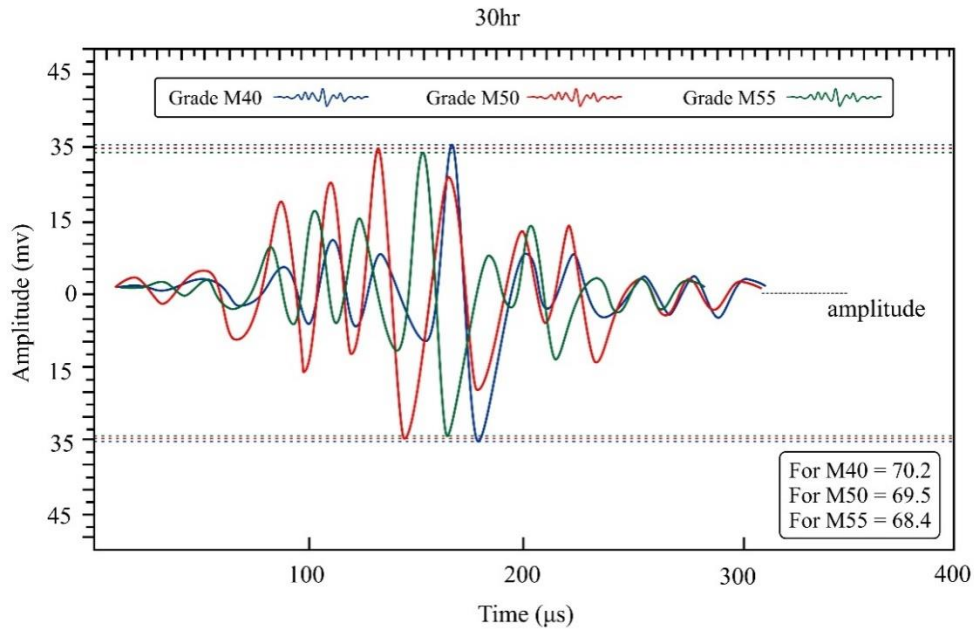

Figure 4.7: Waves recorded at 30hr

At 30hr, maximum amplitude 70.2 was recorded for grade M40 and minimum amplitude of 68.4 was recorded for grade M55. Amplitude on M50 was 69.5. The corrosion was distributing more rapidly on grade M40 than other two grades.
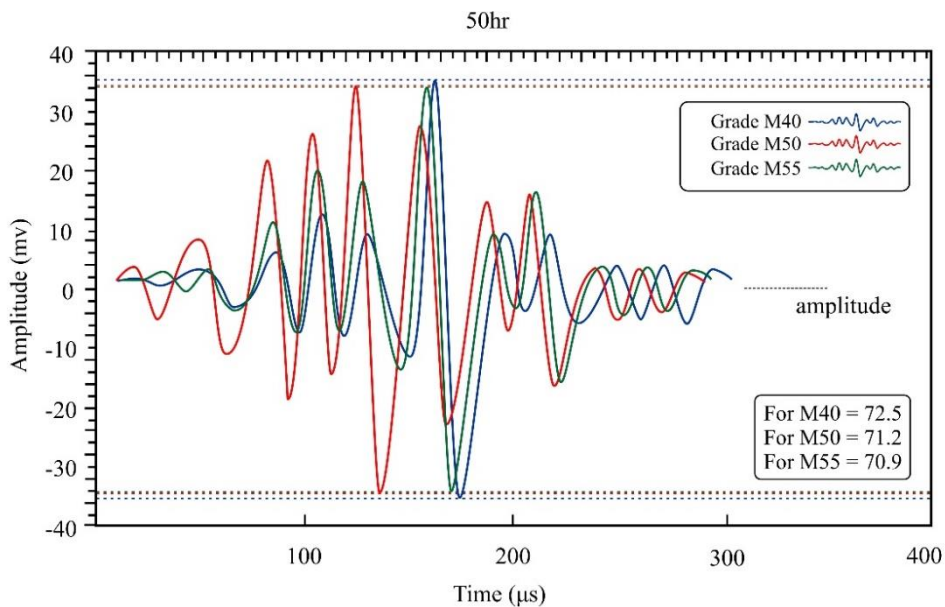

Figure 4.8: Waves recorded at 50hr

At 50hr, maximum amplitude 72.5 was recorded for grade M40 and minimum amplitude of 70.9 was recorded for grade M55. Amplitude recorded on M50 was 71.2. Grade M40 showed unproductive results among three grades. And from the amplitude data it can be conclude that Grade M50 showed the minimum deflection throughout the monitoring because of its better material composition, because of which it leads to a surpassing performance during corrosion acceleration period among the tested grades. Increase of amplitude versus time for M40, M50 and M55 grades are shown in the Figure 4.9.
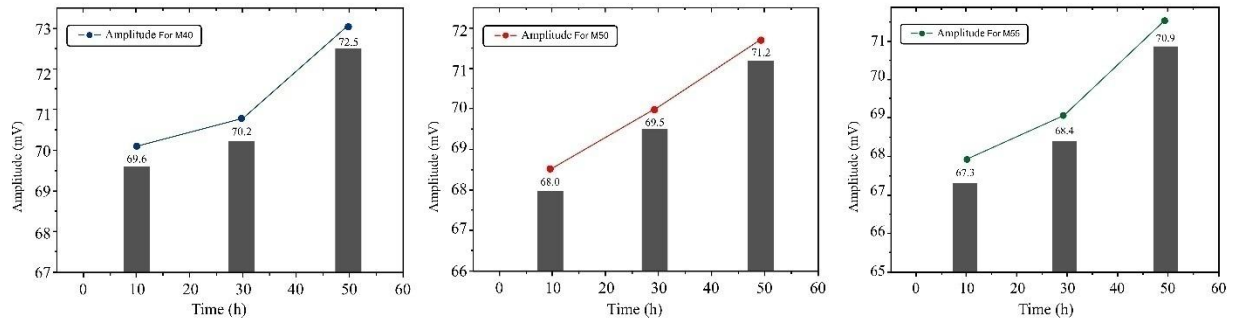

Figure 4.9: Increase of amplitude versus time

At about approximate 50-60hr, the amplitude stopped increasing and the wave propagation from steel bar to concrete gave similar results (as shown in Figure 4.10). Thus, the amplitude of the wave that we got at 50h showed the initiation of corrosion. Thus, the initiation of the corrosion and the cracking of the concrete could detect through amplitude of the wave. It should also be noted that the conducted experiments had very good repeatability.
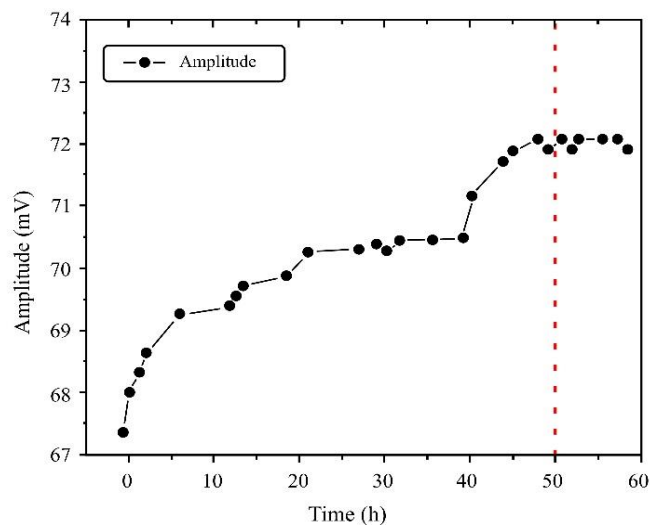

Figure 4.10: Increase of amplitude versus time for all grades

67

4.4 Comparison results

4.4.1 Compression Test comparison

From compression test it can be concluded that Grade M55 showed better compression strength after curing of 28 days. Hence M55 grade can preferred over other two grades.

Day 28		
M40	**M50**	**M55**
46.83 Mpa	54.38Mpa	58.57Mpa

4.4.2 Corrosion Test comparison

From corrosion monitoring test it can be concluded that Grade M55 is more ideal for work under in corroded scenario. Hence M55 grade can preferred over M40 & M55 grades.

50 hr		
M40	**M50**	**M55**
72.5 mV	71.2 mV	70.2 mV

4.5 Concluding remarks

This chapter has introduced a new and easy approach for tracking the practice of corrosion in RC structures directly from initiation into rebar corrosion extracted from the admittance signatures of PZT patches surface-bonded into the years. The admittance worth of three distinct ranges was compared. The suggested strategy is non-destructive in character and entirely autonomous. The impedance-based method of corrosion tracking by using the PZT patch can be used in corrosion of rebars in real-life RC constructions, where they aren't subjected to a direct visual analysis. To validate the nature of changes emphasized by the amplitude signature information, corrosion tracking results using the electromechanical impedance procedure, representative samples of each grade were compared. The amplitude values for every single concrete column of different levels were analyzed to discover the best appropriate work samples in actual scenarios. From the tests, Grade M55 is more practically suitable for both compression wise and applications which are more prone to corrosion.

CHAPTER 05
CONCLUSIONS AND FUTURE SCOPE

5.1 General

The main objective of this research was to monitor the corrosion expansion in the steel rebar from RC structures by using electro mechanical technique (with the help of PZT sensors). The piezoelectric sensor includes two conductive piezoelectric components that are employed for producing and receiving ultrasonic waves along with steel bar. The growth of these corrosion products altered the wave amplitude. Also, the wave propagation from steel bar of concrete gave similar results as the amplitude keeps increasing.

The uniqueness at this thesis is the very first time an inclusive study on the use of their comparable structural parameters such as corrosion monitoring in concrete structures of different grades are researched and related corrosion assessment models are developed. This chapter provides ideas about future work which will match the material and draws conclusions.

5.2 Research outcomes

The final research results of the thesis mainly include the creation of a comparative data of compression test results and corrosion detection results of different grades. And to compare them for future reference for better implementation in real structural applications. Important results and outcomes of research are outlined as follows:

- In this research work we have used Grade-43 cement and M40, M50 and M55 grade of concrete for compression test and corrosion monitoring test.

- To find out the compressive strength of grades (M40, M50 and M55) total 9 cubes of each grade were casted i.e., total 27 cubes were casted. Samples were cured at different time period i.e., 7days, 14 days &28 days. Compressive strength of M40 (46.83 MPa), M50 (54.38 Mpa) and M55 (58.57) was obtained after 28 days of curing.

- For non-destructive corrosion test total 3-3 beam i.e. total 9 beams were casted of all three grades (M40, M50 and M55). In research work, the corrosion rates in high grades of concrete were detected and also which grade is corrosive easily with the help PZT sensor. These sensors include two piezo-sensors which were utilized for producing and receiving amplitude values. Transmission of waves changes due to the growth of corrosion products.

- Throughout initiation of corrosion monitoring test amplitude was started recording at 10hr maximum amplitude 69.6 was listed for grade M40 and minimum amplitude of 67.3 was listed for grade M55. The initiation of corrosion was initially began on grade M40 then in M50 & M55. Therefore, Grade M40 shows maximum deflection during beginning hours of evaluation. The upcoming values of amplitude were taken following a difference of 20-20hr. The corrosion was distributing more quickly on grade M40 compared to other two grades. In 50hr, maximum amplitude 72.5 was listed for grade M40 and minimum amplitude of 70.9 was listed for grade M55. Grade M40 revealed undesirable consequences among three grades. This implies lower grade concrete is far more vulnerable to corrosion.

5.3 Future recommendations

In future researches, following points can be considered for more flexible outcomes in the corrosion monitor study:

- The current study was carried out on only three higher grades of concrete. In future, same research can also be done by using different strength of concrete and by using different grades of steel.

- In this work we have used PZT sensor for corrosion detection but same can be extend with new wireless sensors.

- The corrosion rate model could be used by using other damage identification methods, corrosion for real time structure to could be find to check the long-term effect.

- In future work OPC 43 grade of cement can be replaced with Geopolymer concrete.

From this study and literature reviews, this non-destructive technique, electro mechanical impedance technique by using piezoelectric sensor for corrosion evaluation of different cement grades of concrete has a vast possibility in future. So, at the end we can conclude that this could be a better assessment conventional electrochemical technique.

REFERENCES

[1] Shi, W., Chen, Y., Liu, P. and Xu D., (2019). "Corrosion Investigation of Reinforced Concrete Based on Piezoelectric Smart Materials". *Materials*. 12(3), pp.1-10.

[2] Hansson, Jaffer, S. J., Poursea, A., (2007), "Corrosion of Reinforcing Bars in Concrete", *Portland Cement Association, Skokie, Illinois, USA*, pp. 1-13.

[3] Li, W., Liu, T., Gao, S., Luo, M., Wang, J. and Wu, J., (2019), "An electromechanical impedance-instrumented corrosion-measuring probe". *Journal of Intelligent Material Systems and Structures*, 30(14), pp.2135-2146.

[4] Broomfield, J. P., (2007), "Corrosion of Steel in Concrete, Understanding, Investigation and Repair", *Second edition, Taylor and Francis*.

[5] Dehwah, H.A., Maslehuddin, M. and Austin, S.A., (2002). "Long-term effect of sulfate ions and associated cation type on chloride-induced reinforcement corrosion in Portland cement concretes". *Cement and Concrete Composites*, 24(1), pp.17-25.

[6] Park, S., Yun, C.B., Roh, Y. and Lee, J.J., (2006). "PZT-based active damage detection techniques for steel bridge components". *Smart Materials and Structures*, 15(4), pp.957-966.

[7] Simmers Jr, G.E., (2005). "Impedance-based structural health monitoring to detect corrosion (Doctoral dissertation, Virginia Tech)".

[8] Palit, S., (2018). "Recent advances in corrosion science: a critical overview and a deep comprehension". *In Direct Synthesis of Metal Complexes,* Elsevier, pp. 379-411.

[9] Kansara, D.P., Sorathiya, A.P. and Patel, H.R., (2018). "Corrosion monitoring and detection techniques in petrochemical refineries". *IOSR Journal of Electrical and Electronics Engineering (IOSRJEEE)*, 13(2), pp.85-93.

[10] Birbilis, N., & Hinton, B., (2011). "Corrosion and corrosion protection of aluminium". *Fundamentals of Aluminium Metallurgy,* pp.574–604.

[11] Makhlouf, A. S. H., Herrera, V., & Muñoz, E., (2018). "Corrosion and protection of the metallic structures in the petroleum industry due to corrosion and the techniques for protection". *Handbook of Materials Failure Analysis,* pp.107–122.

[12] Scamans, G. M., Birbilis, N., & Buchheit, R. G., (2010). "Corrosion of Aluminum and its Alloys". *Shreir's Corrosion,* pp.1974.

[13] Ross, C. T. F., (2011). "An overview of pressure vessels under external pressure". *Pressure Vessels,* pp.1–14.

[14] Ahmad, S., (2003). "Reinforcement corrosion in concrete structures, its monitoring and service life prediction—a review". *Cement and Concrete Composites,* 25(4-5), pp.459–471.

[15] Saetta, A. V., Schrefler, B. A., & Vitaliani, R. V., (1993). "The carbonation of concrete and the mechanism of moisture, heat and carbon dioxide flow through porous materials". *Cement and Concrete Research,* 23(4), pp.761–772.

[16] Montemor, M. F, Simoes, A. M. P. and Ferreira, M. G. S., (2003), "Chloride Induced Corrosion on Reinforcing Steel: From the Fundamentals to the Monitoring Technique". *Cement and Concrete Composites*, 25, pp.491-502.

[17] Hussain, S. E., Rasheeduzzafar, A., Musallam, A. Al. and Gahtani A. S. Al., (1995), " Factors Affecting Threshold Chloride for Reinforcement Corrosion in Concrete", *Cement and Concrete Research*, 25(7), pp.1543-1555.

[18] Dhakal, D.R., Neupane, K.E.S.H.A.B., Thapa, C.H.I.R.A.Y.U. and Ramanjaneyulu, G.V., (2013). "Different techniques of structural health monitoring". *Research and Development (IJCSEIERD)*, 3(2), pp.55-66.

[19] Zaki, A., Chai, H.K., Aggelis, D.G. and Alver, N., (2015). "Non-destructive evaluation for corrosion monitoring in concrete: A review and capability of acoustic emission technique". *Sensors*, *15*(8), pp.19069-19101.

[20] François, R., Laurens, S. and Deby, F., (2018). "Corrosion and Its Consequences for Reinforced Concrete Structures*". Elsevier.*

[21] Sørensen, H.E. and Frølund, T., (2002). "Monitoring of Reinforcement Corrosion in Marine Concrete Structures by the Galvanostatic Pulse Method" *.International Conference on Concrete in Marine Environments, Hanoi, Vietnam, Proceedings.*

[22] Manning D.G., Holt F.B., (1980). "Detecting delamination in concrete bridge decks". *Concr. Int*. 2, pp.34–41.

[23] Sohn H., Park G., Wait J.R., Limback N.P., Farrar C.R.,(2004). "Wavelet-based active sensing for delamination detection in composite structures". *Smart Mater. Struct*. ,13, pp.153–160.

[24] Wevers, M. and Surgeon, M., (2000). "Acoustic Emission and Composites". *Comprehensive Composite Materials,* pp.345–357.

[25] Meade, C. L., (2000). "Accelerated corrosion testing". *Metal Finishing.* 98(6), pp.540–545.

[26] Dimitri,V.V., Chernin, L., and Stewart, M.G., (2009). "Experimental and numerical investigation of corrosion-induced cover cracking in reinforced concrete structures". *Journal of Structural Engineering*, 135(4), pp.376 -385.

[27] Ahmad, S., (2009). "Techniques for inducing accelerated corrosion of steel in concrete". *Arabian Journal for Science and Engineering*, 34(2), pp.95.

[28] Park, G., Cudney, H.H. and Inman, D.J., (2000). "An integrated health monitoring technique using structural impedance sensors". *Journal of Intelligent Material Systems and Structures*, 11(6), pp.448-455.

[29] Peairs, D.M., Park, G. and Inman, D.J., (2004). "Improving accessibility of the impedance-based structural health monitoring method". *Journal of Intelligent Material Systems and Structures*, 15(2), pp.129-139.

[30] Montemor, M. F, Simoes, A. M. P. and Ferreira, M. G. S (2003), "Chloride Induced Corrosion on Reinforcing Steel: From the Fundamentals to the Monitoring Technique". *Cement and Concrete Composites*, 25, pp.491-502.

[31] Hey, F., Bhalla, S. and Soh, C.K., (2006). "Optimized parallel interrogation and protection of piezo-transducers in electromechanical impedance technique". *Journal of intelligent material systems and structures*, 17(6), pp.457-468.

[32] Yang, J.W., Zhu, H.P., Yu, J. and Wang, D.S., (2013). "Experimental study on monitoring steel beam local corrosion based on EMI technique". In *Applied Mechanics and Materials*, *Trans Tech Publications Ltd*. 273, pp. 623-627.

[33] Dehwah, H.A., Maslehuddin, M. and Austin, S.A., (2002). "Long-term effect of sulfate ions and associated cation type on chloride-induced reinforcement corrosion in Portland cement concretes". *Cement and Concrete Composites*, *24*(1), pp.17-25.

[34] Li, W., Liu, T., Zou, D., Wang, J. and Yi, T.H., (2019). "PZT based smart corrosion coupon using electromechanical impedance". *Mechanical Systems and Signal Processing*, 129, pp.455-469.

[35] Ai, D., Zhu, H., Luo, H. and Yang, J., (2014). "An effective electromechanical impedance technique for steel structural health monitoring". *Construction and Building Materials*, 73, pp.97-104.

[36] Jang, B. S., & Oh, B. H., (2010). "Effects of non-uniform corrosion on the cracking and service life of reinforced concrete structures". *Cement and Concrete Research*, 40(9), pp.1441–1450.

[37] Almusallam, A.A., (2001)." Effect of degree of corrosion on the properties of reinforcing steel bars". *Construction and building materials*, 15(8), pp.361-368.

[38] El Maaddawy, T.A. and Soudki, K.A., (2003). "Effectiveness of impressed current technique to simulate corrosion of steel reinforcement in concrete". *Journal of materials in civil engineering*, 15(1), pp.41-47.

[39] Baptista, F.G., Vieira Filho, J. and Inman, D.J., (2010). "Sizing PZT transducers in impedance-based structural health monitoring". *IEEE Sensors Journal*, 11(6), pp.1405-1414.

[40] Nakamura, E., Watanabe, H., Koga, H., Nakamura, M. and Ikawa, K., (2008). "Half-cell potential measurements to assess corrosion risk of reinforcement steels in a PC bridge". In *RILEM symposium on on site assessment of concrete, masonry and timber structures-SACoMaTiS* .pp.109-117.

[41] Ghaz. M. P., Lagor. O. B. and Ghoda. P., (2009), "Quantitative Interpretation of Half-Cell Potential Measurements in Concrete Structures", *Journal of Materials in Civil Engineering, ASCE*, 21(9), pp.467-475.

[42] Bhalla, S., Vittal, A. P. R. and Veljkovic, M., (2012), "Piezo-Impedance Transducers for Residual Fatigue Life Assessment of Bolted Steel Joints". *Journal of Structural Health Monitoring*, 11(6), pp.733-750.

[43] Rathod, N.G.S.M., and Moharana, N.C., (2015), "Advanced methods of corrosion monitoring". *International Journal of Research in Engineering and Technology*, 4(1), pp.413-420.

[44] Altoubat, S., Maalej, M., and Shaikh, F.U.A., (2016). "Laboratory Simulation of Corrosion Damage in Reinforced Concrete". *International Journal of Concrete Structures and Materials,* 10(3), pp.383–391.

[45] Bhalla, S. and Soh, C.K., (2004). "Structural health monitoring by piezo-impedance transducers. I: Modeling". *Journal of Aerospace Engineering*, 17(4), pp.154-165.

[46] Bhalla, S. and Soh, C.K., (2004). "Structural health monitoring by piezo–impedance transducers. II: applications". *Journal of Aerospace Engineering*, 17(4), pp.166-175.

[47] Park, S. and Park, S.K., (2010). "Quantitative corrosion monitoring using wireless electromechanical impedance measurements". *Research in Nondestructive Evaluation*, 21(3), pp.184-192.

[48] Moreno, M., Morris, W., Alvarez, M.G. and Duffó, G.S., (2004). "Corrosion of reinforcing steel in simulated concrete pore solutions: effect of carbonation and chloride content". *Corrosion Science*, 46(11), pp.2681-2699.

[49] Santhakumar, A.R., (2007). "Concrete Technology", *Oxford University Press*.48

[50] Shetty, M.S., (2005). "Concrete Technology-Theory and Practice", S. Chand and Co.

[51] IS 2386(Part 1):1963, "Methods of test for aggregates for concrete: Part 1 Particle size and shape, Jan 2007

[52] IS 383: 1970, "Indian standard Specifications for coarse and fine aggregates from natural sources for concrete", *Bureau of Indian Standards,* New Delhi.

[53] IS 8112: 1989, "43 grade ordinary Portland cement-specification", *Bureau of Indian Standards,* New Delhi.

[54] IS: 4031-1988, "Methods for Physical Tests for Hydraulic Cement", *Bureau of Indian Standards,* New Delhi.

[55] IS: 9103-1999, "Specification for Concrete Admixtures", *Bureau of Indian Standards,* New Delhi.

[56] Talakokula, V., Bhalla, S., Bhattacharjee, B. and Gupta, A., (2015). "Non-destructive assessment of rebar corrosion using peizo-transducers using equivalent structural parameters". *Research Gate,* pp.1-38.

[57] Qin, L., Qin, Q., Ren, H., Dong, B. and Xing, F., (2014). "Corrosion monitoring using embedded piezoelectric sensors". *The Open Civil Engineering Journal*, 8(1).

[58] Dowson, A.J., (1981). "Mix design for concrete block paving". *Precast Concrete*, 12, pp.65.

[59] IS 10262: 1982, "Recommended guidelines for concrete mix design", *Bureau of Indian Standards,* New Delhi.

[60] IS 4031: Part 4: 1988, "Methods of physical tests for hydraulic cement: Part 4 Determination of consistency of standard cement paste". *Bureau of Indian Standards, New Delhi, India.*

[61] IS 4031: Part 5: 1988, "Methods of physical tests for hydraulic cement: Part 5 Determination of initial and final setting time". *Bureau of Indian Standards, New Delhi, India.*

[62] IS 516: 1959, "Methods of tests for strength of concrete", *Bureau of Indian Standards*, New Delhi.

[63] Park, G., Inman, D. J., Farrar, C. R., (2003a), "Recent Studies in Piezoelectric Impedance-Based Structural health Monitoring", Proceedings of 4th International Workshop on Structural Health Monitoring, edited by F. K. Chang.

[64] Bhalla, (2004), "A Mechanical Impedance Approach for Structural Identification, Health Monitoring and Non-Destructive Evaluation Using Piezo-Impedance Transducers", *PhD Thesis, School of Civil and Environmental Engineering, Nanyang Technological University*, Singapore.

[65] Ahmad, S., (2009). "Techniques for inducing accelerated corrosion of steel in concrete". *Arabian Journal for Science and Engineering*, 34(2), pp.95.

[66] Zhou, S., Liang, C. and Rogers, C. A., (1995), "Integration and Design of Piezoceramic Elements in Intelligent Structures", *Journal of Intelligent Material Systems and Structures*, 6 (6), pp.733-743.

JOURNAL PUBLICATION

[1] Thakur, A. and Saurav, (2020), "A Review Paper on Early-Stage Corrosion Detection in Reinforced Concrete Structure with Piezo-Electric Sensor", *Test Engineering and Management*, *The Mattingley Publishing Co., Inc. USA*, Vol. 82, pp- 9973-9985. [**Scopus Indexed**]

JAYPEE UNIVERSITY OF INFORMATION TECHNOLOGY, WAKNAGHAT
PLAGIARISM VERIFICATION REPORT

Date: 26/5/2020

Type of Document (Tick): [PhD Thesis] [M.Tech Dissertation/ Report] ✓ [B.Tech Project Report] [Paper]

Name: AISHWARYA THAKUR Department: CIVIL ENG Enrolment No 182652

Contact No. _____ E-mail. ishu.thakur109@gmail.com

Name of the Supervisor: DY. SAURAV

Title of the Thesis/Dissertation/Project Report/Paper (In Capital letters): REAL TIME CORROSION MONITORING OF STEEL BARS EMBEDDED IN CONCRETE USING PIEZO-ELECTRIC SENSORS

UNDERTAKING

I undertake that I am aware of the plagiarism related norms/ regulations, if I found guilty of any plagiarism and copyright violations in the above thesis/report even after award of degree, the University reserves the rights to withdraw/revoke my degree/report. Kindly allow me to avail Plagiarism verification report for the document mentioned above.

Complete Thesis/Report Pages Detail:
- Total No. of Pages = 71
- Total No. of Preliminary pages = 13
- Total No. of pages accommodate bibliography/references = 78

(Signature of Student)

FOR DEPARTMENT USE

We have checked the thesis/report as per norms and found Similarity Index at ....9........(%). Therefore, we are forwarding the complete thesis/report for final plagiarism check. The plagiarism verification report may be handed over to the candidate.

(Signature of Guide/Supervisor)
26/5/2020

Signature of HOD
HOD
CE DEPT

FOR LRC USE

The above document was scanned for plagiarism check. The outcome of the same is reported below:

Copy Received on	Excluded	Similarity Index (%)	Generated Plagiarism Report Details (Title, Abstract & Chapters)	
			Word Counts	
Report Generated on	• All Preliminary Pages • Bibliography/Images/Quotes • 14 Words String		Character Counts	
		Submission ID	Total Pages Scanned	
			File Size	

Checked by
Name & Signature

Librarian